

*Midwest State's Regional Pooled Fund Research Program
Fiscal Year 1998-1999 (Year 9)
Research Project Number SPR-3(017)*

CRASH TESTING OF MISSOURI'S W-BEAM TO THRIE-BEAM TRANSITION ELEMENT

Submitted by

Karla A. Polivka, B.S.M.E., E.I.T.
Research Associate Engineer

Ronald K. Faller, Ph.D., P.E.
Research Assistant Professor

Dean L. Sicking, Ph.D., P.E.
Associate Professor and MwRSF Director

John D. Reid, Ph.D.
Associate Professor

John R. Rohde, Ph.D., P.E.
Associate Professor

James C. Holloway, M.S.C.E., E.I.T.
Research Associate Engineer

MIDWEST ROADSIDE SAFETY FACILITY

University of Nebraska-Lincoln
1901 "Y" Street, Building "C"
Lincoln, Nebraska 68588-0601
(402) 472-6864

Submitted to

MIDWEST STATE'S REGIONAL POOLED FUND PROGRAM

Nebraska Department of Roads
1500 Nebraska Highway 2
Lincoln, Nebraska 68502

MwRSF Research Report No. TRP-03-94-00

September 12, 2000

Technical Report Documentation Page

1. Report No. SPR-3(017)		2.		3. Recipient's Accession No.	
4. Title and Subtitle Crash Testing of Missouri's W-Beam to Thrie Beam Transition Element				5. Report Date September 12, 2000	
				6.	
7. Author(s) Polivka, K.A., Faller, R.K., Reid, J.D., Sicking, D.L., Rohde, J.R., and Holloway, J.C.				8. Performing Organization Report No. TRP-03-94-00	
9. Performing Organization Name and Address Midwest Roadside Safety Facility (MwRSF) University of Nebraska-Lincoln 1901 Y St., Bldg. C Lincoln, NE 68588-0601				10. Project/Task/Work Unit No.	
				11. Contract © or Grant (G) No. SPR-3(017)	
12. Sponsoring Organization Name and Address Midwest States Regional Pooled Fund Program Nebraska Department of Roads 1500 Nebraska Highway 2 Lincoln, Nebraska 68502				13. Type of Report and Period Covered Final Report 1998-2000	
				14. Sponsoring Agency Code	
15. Supplementary Notes Prepared in cooperation with U.S. Department of Transportation, Federal Highway Administration.					
16. Abstract (Limit: 200 words) <p>For longitudinal barriers, it is common practice to use standard W-beam guardrail along the required highway segments and to use a stiffened thrie beam guardrail in a transition region near the end of a bridge. As a result of the differences in rail geometries, a W-beam to thrie beam transition element is typically used to connect the two rail sections as well as to provide continuity in the barrier system. However, the W-beam to thrie beam transition element has not been evaluated according to current impact safety standards. Therefore, an approach guardrail transition system, including a W-beam to thrie beam transition element, was constructed and crash tested. The transition system was attached to Missouri's thrie beam and channel bridge railing system.</p> <p>The research study included full-scale vehicle crash testing, using a small car and a ¼-ton pickup truck. The first test, with a small car impacting at a speed of 99.5 km/hr and an angle of 25.7 degrees, was successful as the vehicle was safely redirected. The second test, with a ¼-ton pickup truck impacting at a speed of 98.3 km/hr and an angle of 25.3 degrees, was unsuccessful as the vehicle pocketed in the rail and then rolled onto its side. The tests were conducted and reported in accordance with the requirements specified in NCHRP Report No. 350, <i>Recommended Procedures for the Safety Performance Evaluation of Highway Features</i>. The safety performance of the W-beam to thrie beam transition element was determined to be unacceptable according to Test Level 3 (TL-3) of the NCHRP Report No. 350 criteria.</p>					
17. Document Analysis/Descriptors Highway Safety, Guardrail, Longitudinal Barrier, W-Thrie Transition,				18. Availability Statement No restrictions. Document available from: National Technical Information Services, Springfield, Virginia 22161	
19. Security Class (this report) Unclassified		20. Security Class (this page) Unclassified		21. No. of Pages 111	22. Price

DISCLAIMER STATEMENT

The contents of this report reflect the views of the authors who are responsible for the facts and the accuracy of the data presented herein. The contents do not necessarily reflect the official views or policies of the State Highway Departments participating in the Midwest State's Regional Pooled Fund Research Program nor the Federal Highway Administration. This report does not constitute a standard, specification, or regulation.

ACKNOWLEDGMENTS

The authors wish to acknowledge several sources that made this project possible: (1) the Midwest States Regional Pooled Fund Program funded by the Iowa Department of Transportation, Kansas Department of Transportation, Minnesota Department of Transportation, Missouri Department of Transportation, Nebraska Department of Roads, Ohio Department of Transportation, South Dakota Department of Transportation, and Wisconsin Department of Transportation for sponsoring this project; (2) MwRSF personnel for constructing the barriers and conducting the crash tests; and (3) the University of Nebraska-Lincoln for matching support.

A special thanks is also given to the following individuals who made a contribution to the completion of this research project.

Midwest Roadside Safety Facility

K.L. Krenk, B.S.M.A., Shop Manager
E.A. Keller, B.S.M.E., E.I.T., Research Associate Engineer
K.H. Addink, B.S.C.E., Research Associate Engineer
M.L. Hanau, Laboratory Mechanic I
D.M. McBride, Laboratory Mechanic I
Undergraduate and Graduate Assistants

Iowa Department of Transportation

David Little, P.E., Deputy Director, Engineering Division
Jay Chiglo, P.E., Design Methods Engineer

Kansas Department of Transportation

Ron Seitz, P.E., Road Design Squad Leader

Minnesota Department of Transportation

Ron Cassellius, Research Program Coordinator

Missouri Department of Transportation

Vince Imhoff, P.E., Contract Administration Engineer
Tom Allen, P.E., Research and Development Engineer

Nebraska Department of Roads

Leona Kolbet, Research Coordinator

Ken Sieckmeyer, Transportation Planning Manager

Ohio Department of Transportation

Monique Evans, P.E., Roadway Standards Engineer

South Dakota Department of Transportation

David Huft, Research Engineer

Wisconsin Department of Transportation

Rory Rhinesmith, P.E., Chief Roadway Development Engineer

Peter Amakobe, Standards Development Engineer

Dunlap Photography

James Dunlap, President and Owner

TABLE OF CONTENTS

	Page
TECHNICAL REPORT DOCUMENTATION PAGE	i
DISCLAIMER STATEMENT	ii
ACKNOWLEDGMENTS	iii
TABLE OF CONTENTS	v
List of Figures	vii
List of Tables	ix
1 INTRODUCTION	1
1.1 Problem Statement	1
1.2 Research Objective	2
1.3 Scope	2
2 LITERATURE REVIEW	4
3 TEST REQUIREMENTS AND EVALUATION CRITERIA	7
3.1 Test Requirements	7
3.2 Evaluation Criteria	7
4 BARRIER DESIGN DETAILS	10
5 TEST CONDITIONS	24
5.1 Test Facility	24
5.2 Vehicle Tow and Guidance System	24
5.3 Test Vehicles	24
5.4 Data Acquisition Systems	32
5.4.1 Accelerometers	32
5.4.2 Rate Transducer	32
5.4.3 High-Speed Photography	33
5.4.4 Pressure Tape Switches	34
6 COMPUTER SIMULATION	37
6.1 Background	37
6.2 BARRIER VII Results	37

7 CRASH TEST NO. 1	38
7.1 Test MWT-1	38
7.2 Test Description	38
7.3 Barrier Damage	39
7.4 Vehicle Damage	40
7.5 Occupant Risk Values	41
7.6 Discussion	41
8 CRASH TEST NO. 2	58
8.1 Test MWT-2	58
8.2 Test Description	58
8.3 Barrier Damage	60
8.4 Vehicle Damage	61
8.5 Occupant Risk Values	61
8.6 Discussion	62
9 SUMMARY AND CONCLUSIONS	81
10 RECOMMENDATIONS	84
11 REFERENCES	85
12 APPENDICES	87
APPENDIX A - Typical BARRIER VII Input File	88
APPENDIX B - Accelerometer Data Analysis, Test MWT-1	94
APPENDIX C - Rate Transducer Data Analysis, Test MWT-1	101
APPENDIX D - Accelerometer Data Analysis, Test MWT-2	103
APPENDIX E - Rate Transducer Data Analysis, Test MWT-2	110

List of Figures

	Page
1. Installation Layout	12
2. Installation Layout and Design Details	13
3. Design Details	14
4. Design Details (Continued)	15
5. Design Details (Continued)	16
6. Design Details (Continued)	17
7. Thrie Beam and Channel Bridge Rail Design Details	18
8. Thrie Beam and Channel Bridge Rail Design Details (Continued)	19
9. W-beam to Thrie Beam Transition	20
10. W-beam to Thrie Beam Transition (Continued)	21
11. W-beam to Thrie Beam Transition (Continued)	22
12. W-beam to Thrie Beam Transition (Continued)	23
13. Test Vehicle, Test MWT-1	25
14. Vehicle Dimensions, Test MWT-1	26
15. Test Vehicle, Test MWT-2	28
16. Vehicle Dimensions, Test MWT-2	29
17. Vehicle Target Locations, Test MWT-1	30
18. Vehicle Target Locations, Test MWT-2	31
19. Location of High-Speed Cameras, Test MWT-1	35
20. Location of High-Speed Cameras, Test MWT-2	36
21. Summary of Test Results and Sequential Photographs, Test MWT-1	43
22. Additional Sequential Photographs, Test MWT-1	44
23. Documentary Photographs, Test MWT-1	45
24. Documentary Photographs, Test MWT-1	46
25. Documentary Photographs, Test MWT-1	47
26. Impact Location, Test MWT-1	48
27. Final Vehicle Position, Test MWT-1	49
28. W-beam to Thrie Beam Transition Damage, Test MWT-1	50
29. W-beam to Thrie Beam Transition Damage, Test MWT-1	51
30. Post Nos. 7 and 8 Damage, Test MWT-1	52
31. Wooden Blockout Damage, Test MWT-1	53
32. Permanent Set Deflections, Test MWT-1	54
33. Vehicle Damage, Test MWT-1	55
34. Vehicle Damage, Test MWT-1	56
35. Occupant Compartment Deformations, Test MWT-1	57
36. Summary of Test Results and Sequential Photographs, Test MWT-2	63
37. Additional Sequential Photographs, Test MWT-2	64
38. Additional Sequential Photographs, Test MWT-2	65
39. Documentary Photographs, Test MWT-2	66
40. Documentary Photographs, Test MWT-2	67

41. Documentary Photographs, Test MWT-2	68
42. Impact Location, Test MWT-2	69
43. Final Vehicle Position, Test MWT-2	70
44. W-beam to Thrie Beam Transition Damage, Test MWT-2	71
45. W-beam to Thrie Beam Transition Damage, Test MWT-2	72
46. W-beam to Thrie Beam Transition Damage, Test MWT-2	73
47. Post Nos. 4 and 5 Damage, Test MWT-2	74
48. Post No. 6 and 7 Damage, Test MWT-2	75
49. Post Nos. 8, 9, and 12 Damage, Test MWT-2	76
50. Permanent Set Deflections, Test MWT-2	77
51. Vehicle Damage, Test MWT-2	78
52. Vehicle Damage, Test MWT-2	79
53. Under-Carriage Vehicle Damage, Test MWT-2	80
B-1. Graph of Longitudinal Deceleration, Test MWT-1	95
B-2. Graph of Longitudinal Occupant Impact Velocity, Test MWT-1	96
B-3. Graph of Longitudinal Occupant Displacement, Test MWT-1	97
B-4. Graph of Lateral Deceleration, Test MWT-1	98
B-5. Graph of Lateral Occupant Impact Velocity, Test MWT-1	99
B-6. Graph of Lateral Occupant Displacement, Test MWT-1	100
C-1. Graph of Roll, Pitch, and Yaw Angular Displacements, Test MWT-1	102
D-1. Graph of Longitudinal Deceleration, Test MWT-2	104
D-2. Graph of Longitudinal Occupant Impact Velocity, Test MWT-2	105
D-3. Graph of Longitudinal Occupant Displacement, Test MWT-2	106
D-4. Graph of Lateral Deceleration, Test MWT-2	107
D-5. Graph of Lateral Occupant Impact Velocity, Test MWT-2	108
D-6. Graph of Lateral Occupant Displacement, Test MWT-2	109
E-1. Graph of Roll, Pitch, and Yaw Angular Displacements, Test MWT-2	111

List of Tables

	Page
1. NCHRP Report 350 Test Level 3 Crash Test Conditions	7
2. NCHRP Report 350 Evaluation Criteria for Crash Tests	9
3. Summary of Safety Performance Evaluation Results - W-beam to Thrie Beam Transition Section	83

1 INTRODUCTION

1.1 Problem Statement

Throughout the U.S., State Highway Departments commonly use standard strong-post, W-beam guardrail systems to prevent errant vehicles from leaving the roadway and encountering safety hazards beyond or near the roadway edge. Although the strong-post, W-beam barriers are generally considered to be flexible systems, it is often necessary to continue the guardrail to the location of a bridge and attach it to a rigid bridge railing system. In order to eliminate the potential for vehicle pocketing or wheel snag at the end of the bridge, a semi-rigid, approach guardrail transition region is added between the flexible guardrail and the rigid bridge rail to provide a more gradual change in lateral barrier stiffness.

Over the years, this change in lateral barrier stiffness has been accomplished with several proven methods, including the use of a reduced post spacing, nesting of the guardrail, placing additional stiffening rails in the region, or combinations thereof. Many of these approach guardrail transition systems have incorporated a thrie beam section as the guardrail element to help meet the increased stiffness requirements or as a result of the bridge railing system using a thrie beam for the rail element. Therefore, a W-beam to thrie beam transition element was developed to account for the differences in rail geometries as well as to provide structural continuity between barrier systems.

Although the field experience of the W-beam to thrie beam section has generally been believed to be acceptable, previous crash testing efforts with passenger-size and small car sedans have been met with mixed results (1-2). While several crash tests on the W-beam to thrie beam section resulted in acceptable performance, other tests resulted in severe wheel snagging and even vehicle roll-over. These crash testing efforts were evaluated according to the guidelines set forth in

NCHRP Report No. 230, *Recommended Procedures for the Safety Performance Evaluation of Highway Appurtenances* (3). As a result, there are several concerns about the performance of the W-beam to thrie-beam transition element, including vehicle under-ride by mini-size vehicles and wheel snagging and rollover of the ¾-ton pickup. Therefore, the W-beam to thrie beam transition element should be crash tested and shown to meet the current impact safety standards set forth in the National Cooperative Highway Research Program (NCHRP) Report No. 350, *Recommended Procedures for the Safety Performance Evaluation of Highway Features* (4) in order for its use to be continued on Federal-aid highways.

1.2 Research Objective

The objective of the research project was to investigate the safety performance of the W-beam to thrie beam transition element used in conjunction with an approach guardrail transition attached to Missouri's thrie beam and channel bridge railing (6). This approach guardrail transition was selected since it was representative of the recently developed thrie beam transitions meeting the NCHRP Report No. 350 impact safety standards. Finally, the W-beam to thrie beam transition element was to be evaluated according to the Test Level 3 (TL-3) safety performance criteria set forth in NCHRP Report No. 350 (4).

1.3 Scope

The research objective was accomplished with a series of tasks. First, a literature review was performed on the previous testing on W-beam to thrie beam transition sections. Second, a barrier system, with a W-beam to thrie beam transition element, was constructed adjacent to an approved approach guardrail transition system. After final fabrication of the test installation, two full-scale vehicle crash tests were performed according to the TL-3 impact conditions of NCHRP Report No.

350. The first test, MWT-1, was performed with a small car, weighing approximately 820 kg, with a target impact speed and angle of 100.0 km/hr and 20 degrees, respectively. The second test, MWT-2, was performed with a ¾-ton pickup truck, weighing approximately 2,000 kg, with a target impact speed and angle of 100.0 km/hr and 25 degrees, respectively. Finally, the test results were analyzed, evaluated, and documented. Conclusions and recommendations were then made that pertain to the safety performance of the W-beam to thrie beam transition element.

2 LITERATURE REVIEW

Previous testing on various W-beam to thrie beam transition sections was conducted by the New York State Department of Transportation (NYSDOT) and was met with mixed results. When the unsymmetrical designs were initially tested with full-size vehicles, the vehicles were forced down under the W-beam rail element, resulting in severe snagging on the lower thrie beam corrugation which included a taper (1-2). In the later tests on a symmetrical W-beam to thrie beam section, two out of the three test vehicles were successfully redirected. Crash testing of the W-beam to thrie beam transition systems previously conducted at NYSDOT were evaluated according to the criteria provided in NCHRP Report No. 230 (3).

NYSDOT performed five full-scale vehicle crash tests on several W-beam to thrie beam transition configurations used to transition from a weak-post, W-beam guardrail system with reduced post spacing to a rigid thrie beam bridge railing. For the first design, an 1.27-m long asymmetrical section was placed between the W-beam and thrie beam rails. At the upstream end of the transition section, the lower corrugation terminated with a 305-mm long taper toward the rail's mid-height. A 2,041-kg passenger-size sedan (test no. 67) impacted the rail 2.67-m upstream from the tapered section at 94.6 km/hr and 25 degrees. During the test, the right-front wheel and suspension severely snagged on the end of the lower thrie beam corrugation, and the test was determined to be unacceptable according to the NCHRP Report No. 230 requirements (3).

Following the failure of test no. 67, the transition section was modified in order to reduce the severe snagging at the end of the section. For the second design, an 1.90-m long asymmetrical section was placed between the W-beam and thrie beam rails. At the upstream end of the transition section, the lower corrugation terminated with an increased taper length of 914 mm, as measured

from the bottom of the rail to the rail's mid-height. A 2,041-kg passenger-size sedan (test no. 68) impacted the rail 1.40-m upstream from the tapered section at 95.8 km/hr and 24 degrees. During the test, the right-front wheel and suspension once again snagged severely on the end of the lower three beam corrugation, and the test was determined to be unacceptable according to the NCHRP Report No. 230 requirements (3).

After the failure of test nos. 67 and 68, the NYSDOT realized that the termination of the lower tapered corrugation presented an insurmountable snag point. Therefore, the W-beam to three beam transition section was redesigned to include a symmetrical tapered section which could adapt W-beam rail directly to three beam rail. This transition section is the same design that now appears in the American Association of State Highway and Transportation Officials' (AASHTO's) *Standard Specifications for Transportation Materials and Methods of Sampling and Testing* (5).

Following the redesign of the symmetrical W-beam to three beam transition section, three additional full-scale crash tests were performed. For this design, a 2,087-kg passenger-size sedan (test no. 69) impacted the rail 2.07-m upstream from the tapered section at 87.5 km/hr and 26 degrees. During the impact, the vehicle was smoothly redirected with only minor snagging on the posts, and the test was determined to be acceptable according to the NCHRP Report No. 230 requirements (3). A fourth test (test no. 70) was performed using an 898-kg small car (Subaru station wagon) impacting the rail 1.07-m upstream from the tapered section at 93.0 km/hr and 20 degrees. During the test, the right-front wheel and bumper snagged severely on the first W6x9 steel post which resulted in the vehicle yawing rapidly away from the rail and rolling onto its side. As a result, the test was determined to be unacceptable according to the NCHRP Report No. 230 requirements (3).

After the failed small car test on the symmetric W-beam to thrie beam transition section, the depth of the steel wide-flange blockouts was increased from 152 mm to 356 mm, and the small car crash test was rerun. This fifth test (test no. 71) was performed using an 816-kg small car (Honda) impacting the rail 0.85-m upstream from the tapered section at 97.0 km/hr and 19 degrees. During the test, the vehicle was smoothly redirected, and the test was determined to be acceptable according to the NCHRP Report No. 230 requirements (3). Although the system was redesigned following the successful test with a passenger-size sedan, a retest with the large car was deemed unnecessary.

Thus, the symmetrical W-beam to thrie beam transition section, combined with 356-mm deep blockouts and used to connect weak-post W-beam guardrail to a thrie approach guardrail transition, met the requirements of NCHRP Report No. 230 (3).

3 TEST REQUIREMENTS AND EVALUATION CRITERIA

3.1 Test Requirements

Longitudinal barriers, such as W-beam to thrie beam transitions, must satisfy the requirements provided in NCHRP Report No. 350 to be accepted for use on new construction projects or as a replacement for existing transition designs not meeting current safety standards. According to Test Level 3 (TL-3) of NCHRP Report No. 350, W-beam to thrie beam transitions must be subjected to two full-scale vehicle crash tests: (1) a 2,000-kg pickup truck impacting at a speed of 100.0 km/hr and at an angle of 25 degrees; and (2) an 820-kg small car impacting at a speed of 100.0 km/hr and at an angle of 20 degrees. The test conditions for TL-3 longitudinal barriers are summarized in Table 1.

Table 1. NCHRP Report 350 Test Level 3 Crash Test Conditions.

Test Designation	Test Vehicle	Impact Conditions		Evaluation Criteria ¹
		Speed (km/hr)	Angle (degrees)	
3-10	820C	100	20	A,D,F,H,I,K,M
3-11	2000P	100	25	A,D,F,K,L,M

¹ - Evaluation criteria explained in Table 2.

3.2 Evaluation Criteria

Evaluation criteria for full-scale vehicle crash testing are based on three appraisal areas: (1) structural adequacy; (2) occupant risk; and (3) vehicle trajectory after collision. Criteria for structural adequacy are intended to evaluate the ability of the barrier to contain, redirect, or allow controlled vehicle penetration in a predictable manner. Occupant risk evaluates the degree of hazard

to occupants in the impacting vehicle. Vehicle trajectory after collision is a measure of the potential for the post-impact trajectory of the vehicle to cause subsequent multi-vehicle accidents. It is also an indicator for the potential safety hazard for the occupants of other vehicles or the occupants of the impacting vehicle when subjected to secondary collisions with other fixed objects. These three evaluation criteria are defined in Table 2. The full-scale vehicle crash tests were conducted and reported in accordance with the procedures provided in NCHRP Report No. 350.

Table 2. NCHRP Report 350 Evaluation Criteria for Crash Tests.

Structural Adequacy	A. Test article should contain and redirect the vehicle; the vehicle should not penetrate, underride, or override the installation although controlled lateral deflection of the test article is acceptable.
Occupant Risk	D. Detached elements, fragments or other debris from the test article should not penetrate or show potential for penetrating the occupant compartment, or present an undue hazard to other traffic, pedestrians, or personnel in a work zone. Deformations of, or intrusions into, the occupant compartment that could cause serious injuries should not be permitted.
	F. The vehicle should remain upright during and after collision although moderate roll, pitching, and yawing are acceptable.
	H. Longitudinal and lateral occupant impact velocities should fall below the preferred value of 9 m/s, or at least below the maximum allowable value of 12 m/s.
	I. Longitudinal and lateral occupant ridedown accelerations should fall below the preferred value of 15 g's, or at least below the maximum allowable value of 20 g's.
Vehicle Trajectory	K. After collision it is preferable that the vehicle's trajectory not intrude into adjacent traffic lanes.
	L. The occupant impact velocity in the longitudinal direction should not exceed 12 m/sec and the occupant ridedown acceleration in the longitudinal direction should not exceed 20 G's.
	M. The exit angle from the test article preferably should be less than 60 percent of test impact angle, measured at time of vehicle loss of contact with test device.

4 BARRIER DESIGN DETAILS

The total length of the installation was 26.67 m. Design details of the W-beam to thrie beam transition element attached to a strong-post, W-beam guardrail and an approach guardrail transition system are provided in Figures 1 through 8. Photographs of the W-beam to thrie beam transition section, the approach guardrail transition, and bridge railing system are shown in Figures 9 through 11. The test installation consisted of four major structural components: (1) two nested 5,715-mm long thrie beam rail sections (each 2.66-mm thick); (2) an 1,905-mm long W-beam to thrie beam transition section (2.66-mm thick); (3) a 15,240-mm long W-beam rail section (2.66-mm thick) attached to a simulated anchorage device; and (4) a 3,810-mm long thrie beam and channel bridge railing system with an attached simulated anchorage device.

The barrier system was constructed with three bridge posts and sixteen guardrail posts, as shown in Figures 1 through 7. Bridge post nos. B1 through B3 were W152x29.8 sections measuring 752-mm long. Post nos. 1 through 5 consisted of galvanized, ASTM A36 steel W152x22.3 sections measuring 2,135-mm long. Post nos. 6 through 8 were W152x13.4 steel sections measuring 1,980-mm long. Post nos. 9 through 14 were also W152x13.4 sections but measuring 1,830-mm long. Post nos. 15 and 16 were timber posts measuring 140-mm wide x 190-mm deep x 1,080-mm long and were placed in steel foundation tubes. The timber posts and foundation tubes were part of an anchorage system used to develop the required tensile capacity of the guardrail at the upstream end of the system. Lap-splice connections between the rail sections were configured to reduce vehicle snagging at the splice during the crash tests.

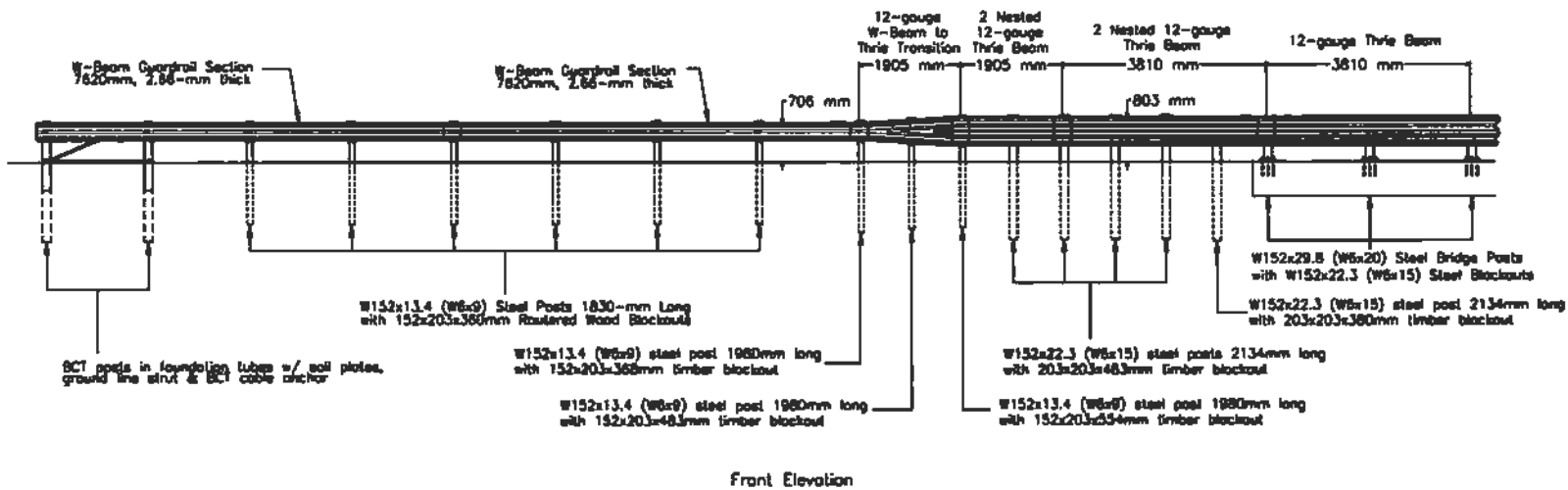
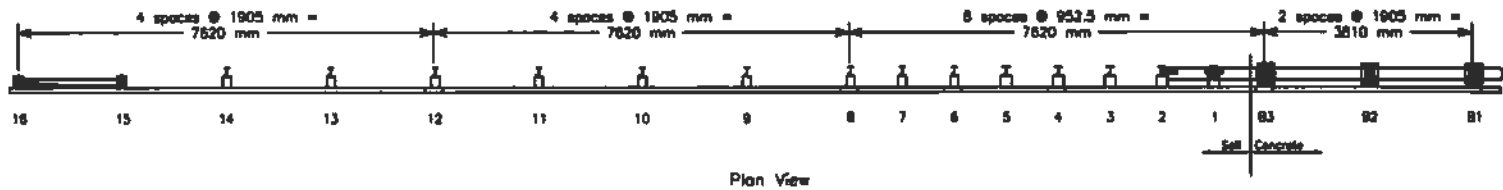
For post no. 1, a wood spacer blockout measuring 203-mm wide x 203-mm deep x 380-mm long was used, as shown in Figure 3. As shown in Figure 4, a wood spacer blockout measuring 203-

mm wide x 203-mm deep x 480-mm long was used for post nos. 2 through 5. At post no. 6, wood spacer blockout measuring 152-mm wide x 203-mm deep x 554-mm long was used, as shown in Figure 5. A 152-mm wide x 203-mm deep x 483-mm long wood spacer blockout was used at post no. 7, as shown in Figure 5. At post nos. 8 through 14, wood spacer blockouts measuring 152-mm wide x 203-mm deep x 360-mm long were used, as shown in Figure 6. For bridge post nos. B1 through B3, ASTM A36 steel W152x22.3 sections measuring 346-mm long were used as blockouts, as shown in Figures 1, 2, and 7.

The spacing between bridge post nos. B1 through B3 was 1,905-mm, as shown in Figure 1. Bridge post no. B3 through guardrail post no. 8 were spaced on 952.5-mm centers. Post nos. 8 through 16 were spaced on 1,905-mm centers, as shown in Figure 1.

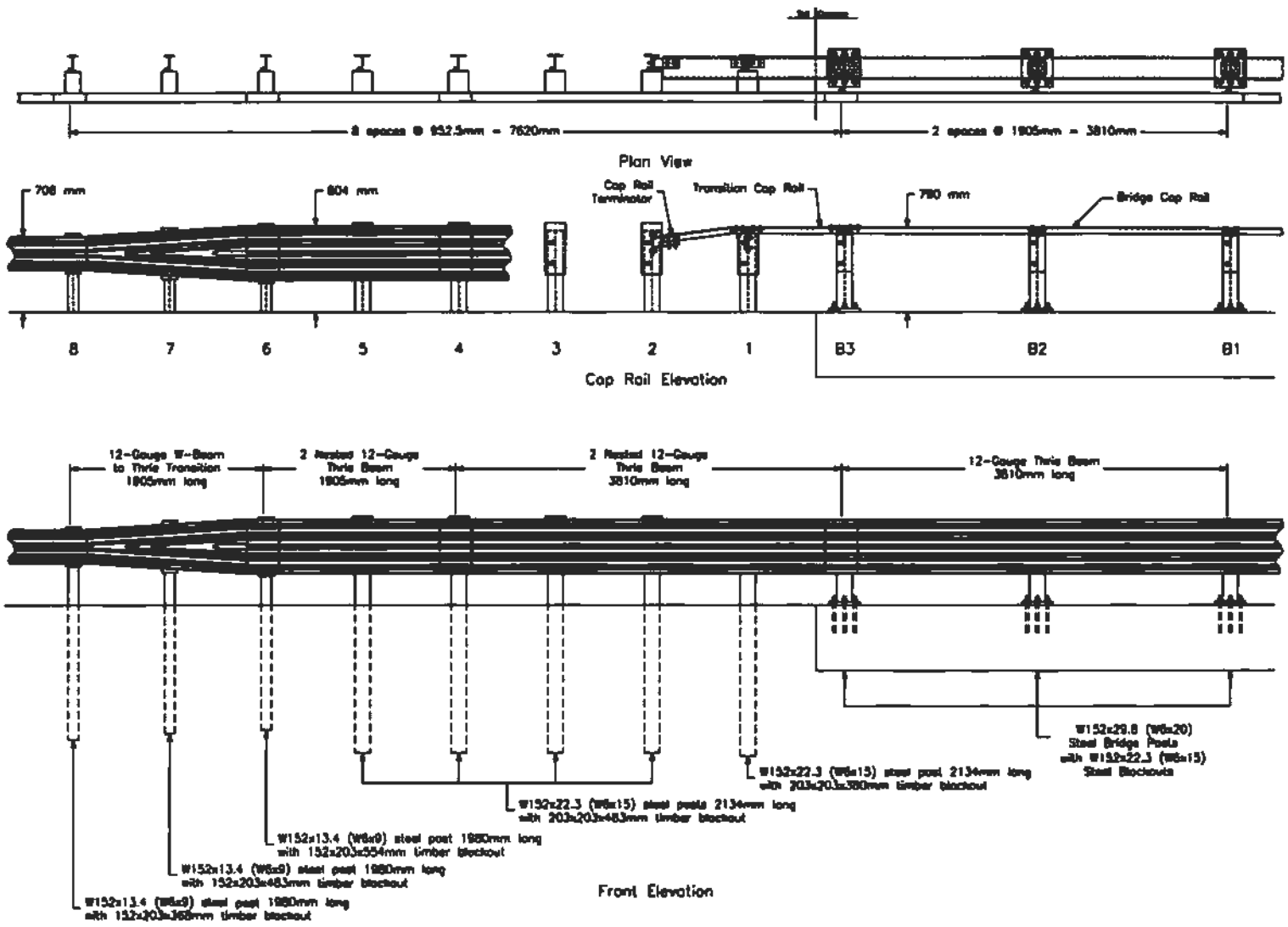
The soil embedment depths for post nos. 1, 2 through 5, 6, 7, 8, and 9 through 14 were 1,403 mm, 1,375 mm, 1,153 mm, 1,189 mm, 1,250 mm, and 1,100 mm, respectively, as shown in Figures 3 through 6. The steel posts were placed in a compacted coarse, crushed limestone material that met Grading B of AASHTO M147-65 (1990) as found in NCHRP Report 350.

The three beam and channel bridge railing system was rigidly attached to the concrete tarmac located at the MwRSF's outdoor test site, as shown in Figures 7, 9, and 12. All construction details for the bridge railing system are provided in Figures 7 through 8. As shown in Figures 9 and 12, a steel anchorage device was attached to the downstream end of the bridge railing to simulate a full-length bridge and to develop the required tensile capacity of the bridge railing system.



12

Figure 1. Installation Layout



13

Figure 2. Installation Layout and Design Details

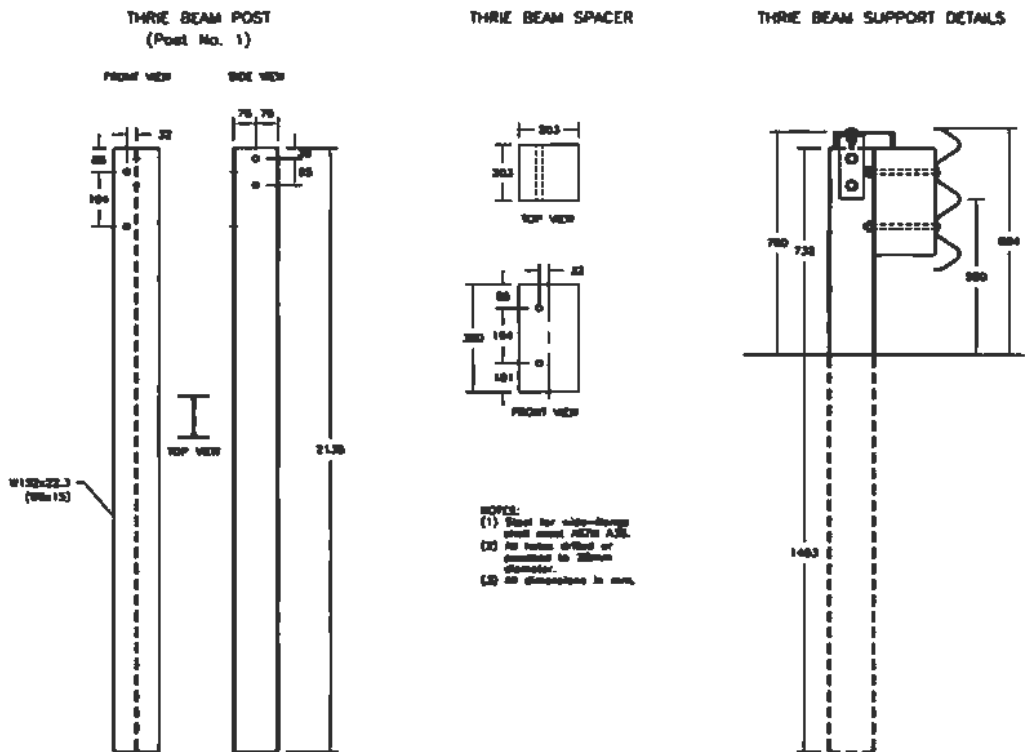
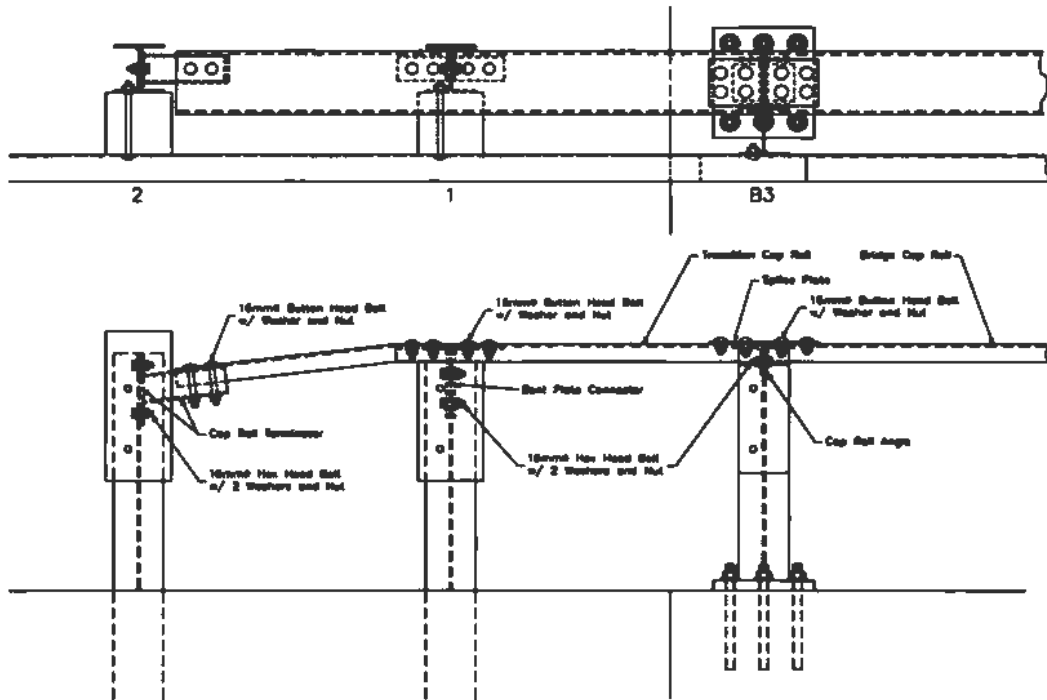
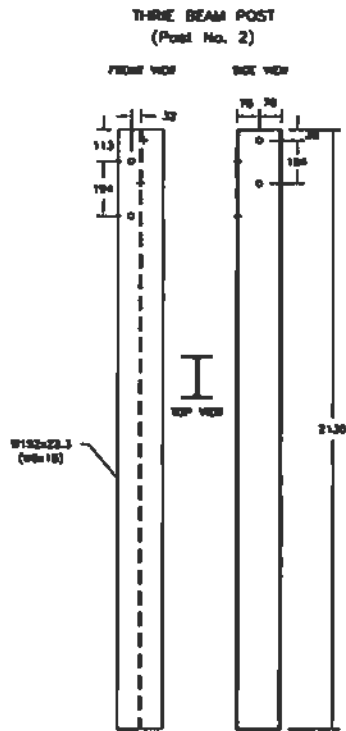
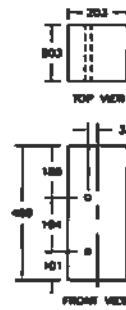


Figure 3. Design Details

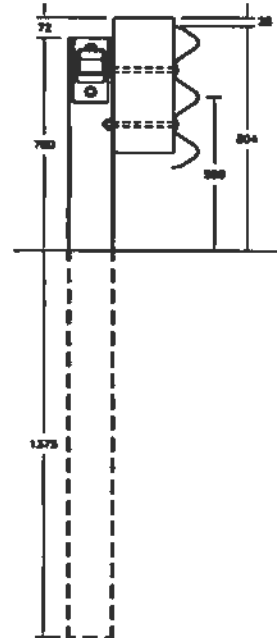


THREE BEAM SPACER

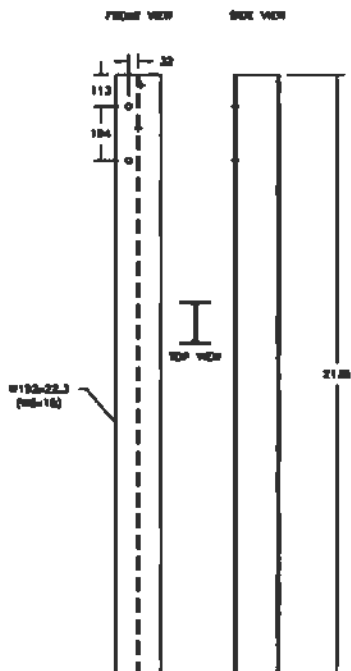


NOTES:
 (1) Steel for shop-erected
 shall meet ASTM A36.
 (2) All holes drilled or
 punched to 1/8" tolerance.
 (3) All dimensions in mm.

THREE BEAM SUPPORT DETAILS



THREE BEAM POSTS
(Post Nos. 3 - 5)



THREE BEAM SPACERS



NOTES:
 (1) Steel for shop-erected
 shall meet ASTM A36.
 (2) All holes drilled or
 punched to 1/8" tolerance.
 (3) All dimensions in mm.

THREE BEAM SUPPORT DETAILS

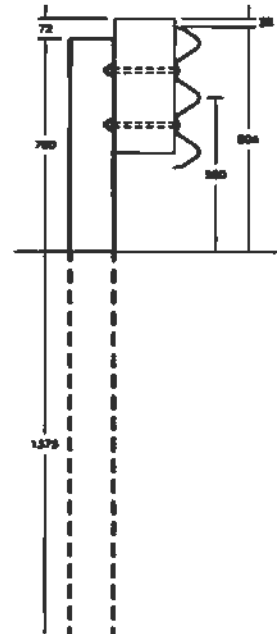


Figure 4. Design Details (Continued)

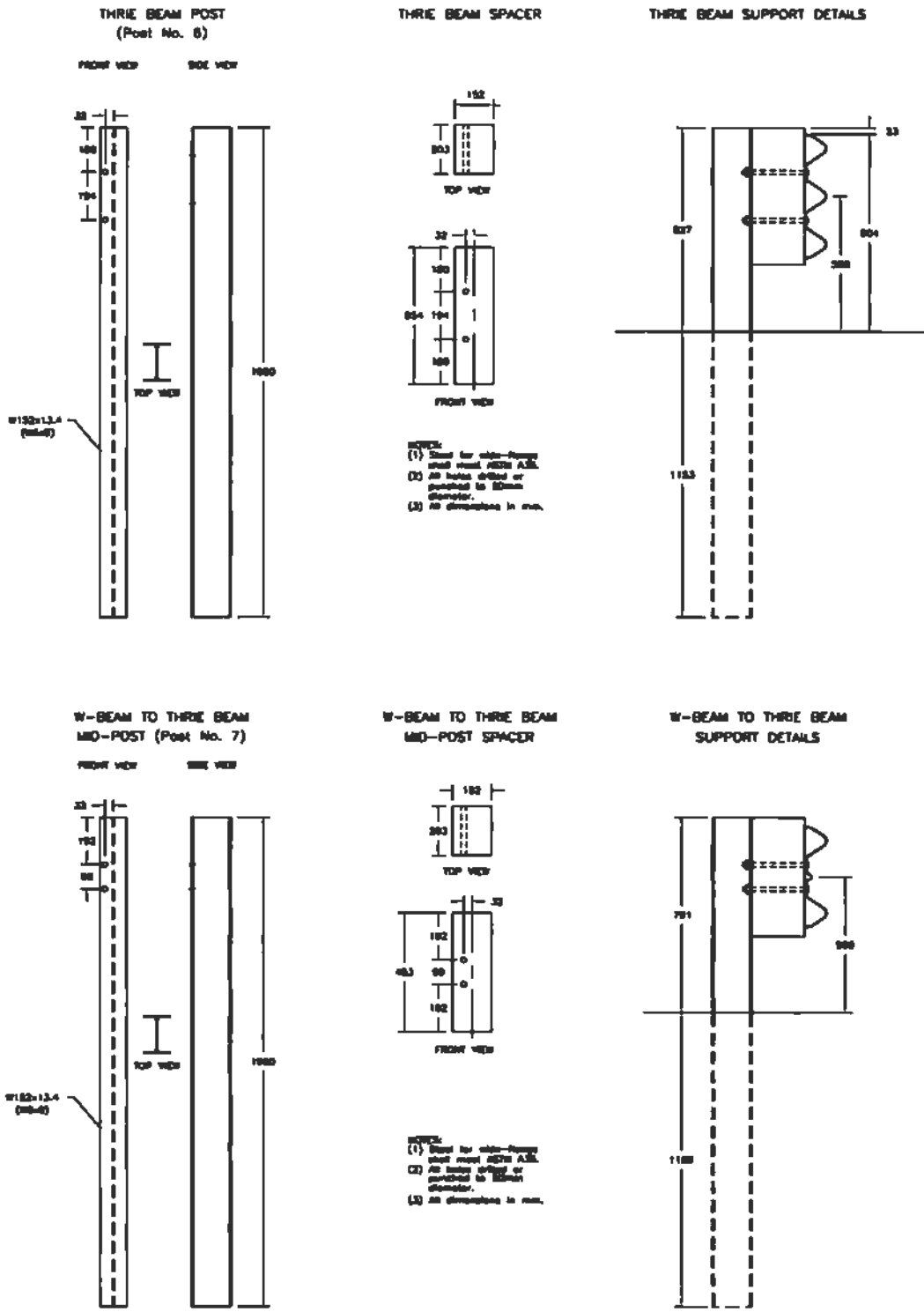
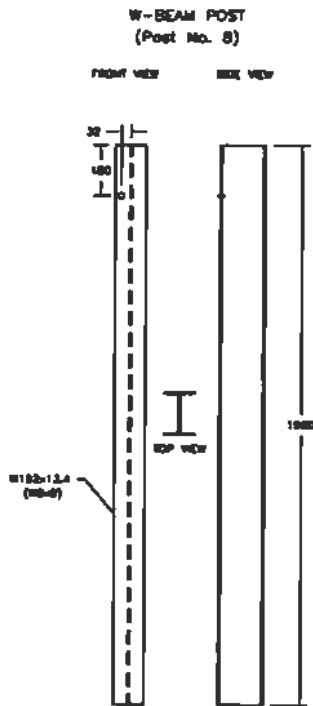


Figure 5. Design Details (Continued)

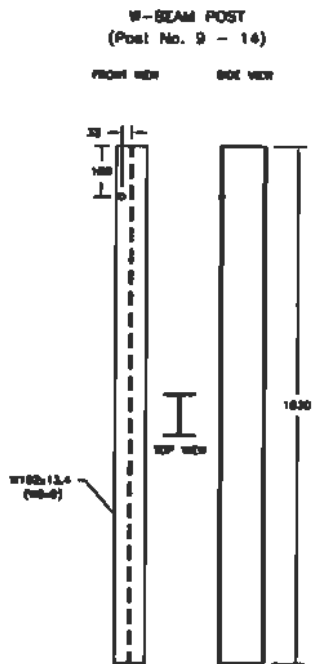
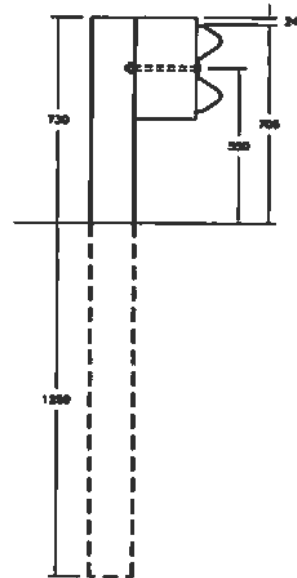


W-BEAM SPACER



- NOTES:**
- (1) Steel for web-panels shall meet ASTM A36.
 - (2) All holes drilled or punched to 3/16 inch diameter.
 - (3) All dimensions in mm.

W-BEAM SUPPORT DETAILS



W-BEAM SPACER



- NOTES:**
- (1) Steel for web-panels shall meet ASTM A36.
 - (2) All holes drilled or punched to 3/16 inch diameter.
 - (3) All dimensions in mm.

W-BEAM SUPPORT DETAILS

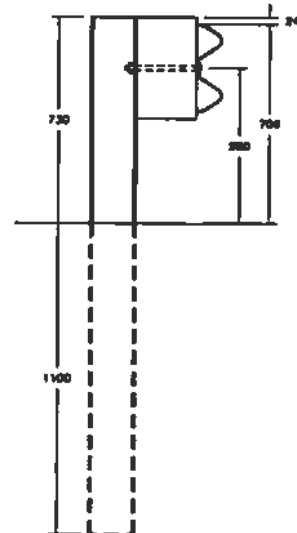
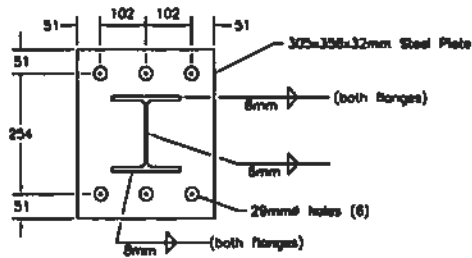
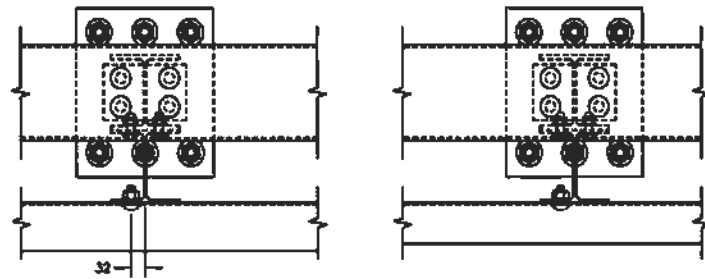


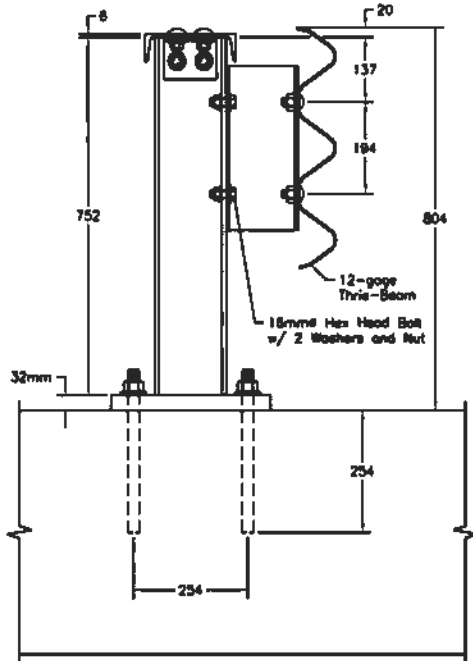
Figure 6. Design Details (Continued)



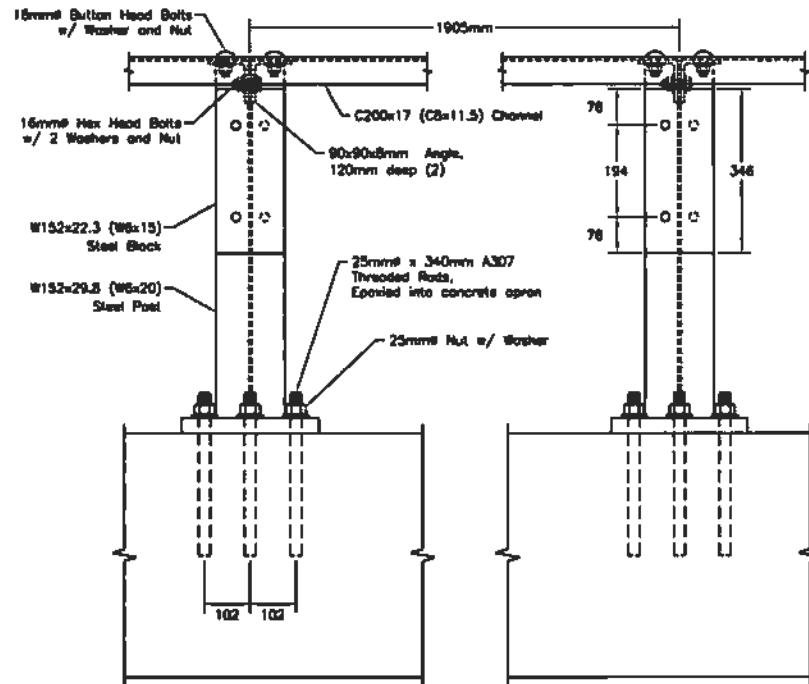
Bridge Connector
 & Post Assembly



TOP VIEW

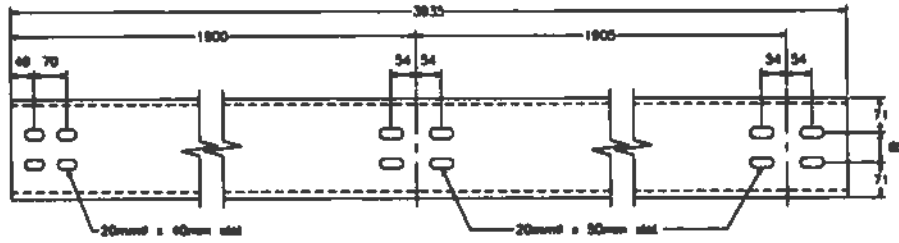


SIDE VIEW

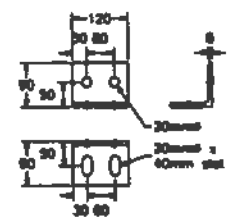


FRONT VIEW
 (Guardrail Omitted)

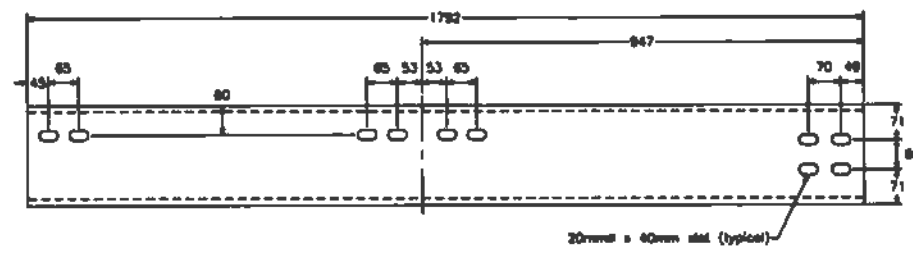
Figure 7. Thrie Beam and Channel Bridge Rail Design Details



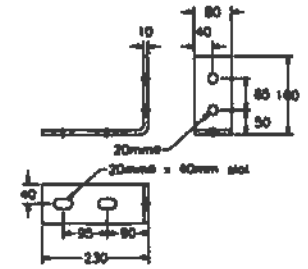
Bridge Cap Rail
C203x17.1 (C8x11.5)



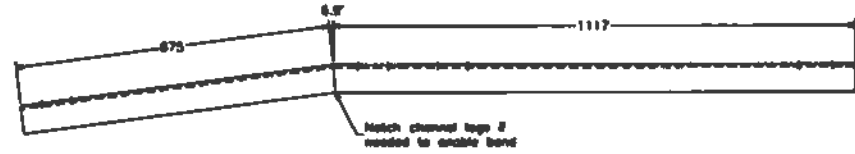
Cap Rail Angle
L 90x90x8mm



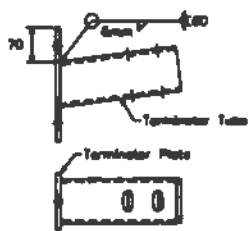
Transition Cap Rail
C203x17.1 (C8x11.5)



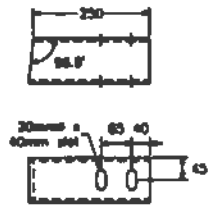
Bent Plate Connector
L 180x230x10mm



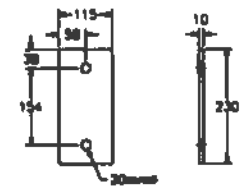
19



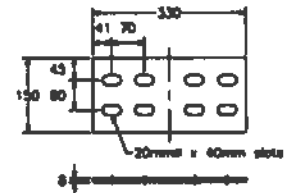
Terminator Assembly



Terminator Tube
TS 90x90x8mm



Terminator Plate
230mm x 115mm x 10mm



Splice Plate
150mm x 330mm x 8mm

Figure 8. Thrie Beam and Channel Bridge Rail Design Details (Continued)



Figure 9. W-beam to Thrie Beam Transition



Figure 10. W-beam to Thrie Beam Transition (Continued)



Figure 11. W-beam to Thrie Beam Transition (Continued)



Figure 12. W-beam to Thrie Beam Transition (Continued)

5 TEST CONDITIONS

5.1 Test Facility

The testing facility is located at the Lincoln Air-Park on the northwest (NW) side of the Lincoln Municipal Airport and is approximately 8.0 km NW of the University of Nebraska-Lincoln. The site is protected by an 2.44-m high chain-link security fence.

5.2 Vehicle Tow and Guidance System

A reverse cable tow system with a 1:2 mechanical advantage was used to propel the test vehicles. The distance traveled and the speed of the tow vehicle are one-half that of the test vehicle. The test vehicle was released from the tow cable before impact with the barrier system. A digital speedometer, located on the tow vehicle, was used to increase the accuracy of the test vehicle impact speed.

A vehicle guidance system developed by Hinch (8) was used to steer the test vehicle. A guide-flag, attached to the front-left wheel and the guide cable, was sheared off before impact. The 9.5-mm diameter guide cable was tensioned to approximately 13.3 kN, and supported by hinged stanchions in the lateral and vertical directions and spaced every 30.48 m initially and at 15.24 m toward the end of the guidance system. The hinged stanchions stood upright while holding up the guide cable, but as the vehicle was towed down the line, the guide-flag struck and knocked each stanchion to the ground.

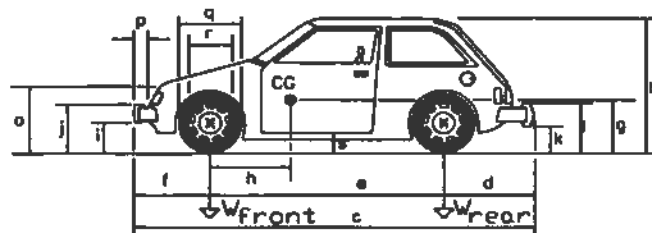
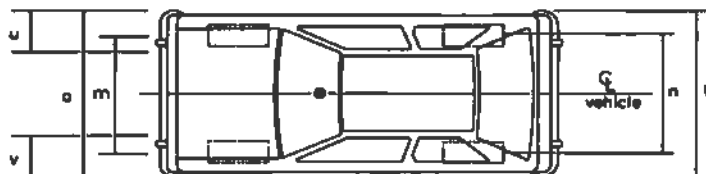
5.3 Test Vehicles

For test MWT-1, a 1993 Ford Festiva was used as the test vehicle. The test inertial and gross static weights were 821 kg and 896 kg, respectively. The test vehicle is shown in Figure 13, and vehicle dimensions are shown in Figure 14.



Figure 13. Test Vehicle, Test MWT-1

Dates: 7/8/99 Test Numbers: MWT-1 Model: Festiva
 Make: Ford Vehicle I.D.#: KNJPT05HQP6146889
 Tire Size: 155 R12 Year: 1993 Odometer: 105942



Vehicle Geometry - mm

a	<u>1562</u>	b	<u>1461</u>
c	<u>3556</u>	d	<u>572</u>
e	<u>2299</u>	f	<u>686</u>
g	<u>546</u>	h	<u>856</u>
i	<u>387</u>	j	<u>521</u>
k	<u>406</u>	l	<u>584</u>
m	<u>1384</u>	n	<u>1391</u>
o	<u>705</u>	p	<u>102</u>
q	<u>546</u>	r	<u>330</u>
s	<u>305</u>	t	<u>1600</u>

height of wheel center 248

Engine Type 4 cyl. gas

Engine size 1.3 L

Transmission Type:

Automatic or Manual
 FWD or RWD or 4WD

Weight - kg	Curb	Test Inertial	Gross Static
W_{front}	<u>512</u>	<u>515</u>	<u>550</u>
W_{rear}	<u>302</u>	<u>306</u>	<u>346</u>
W_{total}	<u>814</u>	<u>821</u>	<u>896</u>

Damage prior to test: NONE

Figure 14. Vehicle Dimensions, Test MWT-1

For test MWT-2, a 1993 GMC 2500 ¾-ton pickup truck was used as the test vehicle. The test inertial and gross static weights were 2,022 kg. The test vehicle is shown in Figure 15, and vehicle dimensions are shown in Figure 16.

The Suspension Method (9) was used to determine the vertical component of the center of gravity for the test vehicles. This method is based on the principle that the center of gravity of any freely suspended body is in the vertical plane through the point of suspension. The vehicle was suspended successively in three positions, and the respective planes containing the center of gravity were established. The intersection of these planes pinpointed the location of the center of gravity. The longitudinal component of the center of gravity was determined using the measured axle weights. The location of the final centers of gravity are shown in Figures 13 through 16.

Square, black and white-checked targets were placed on the vehicle to aid in the analysis of the high-speed film, as shown in Figures 13 through 18. One target was placed on the center of gravity on the driver's side door, the passenger's side door, and on the roof of the vehicle. The remaining targets were located for reference so that they could be viewed from the high-speed cameras for film analysis.

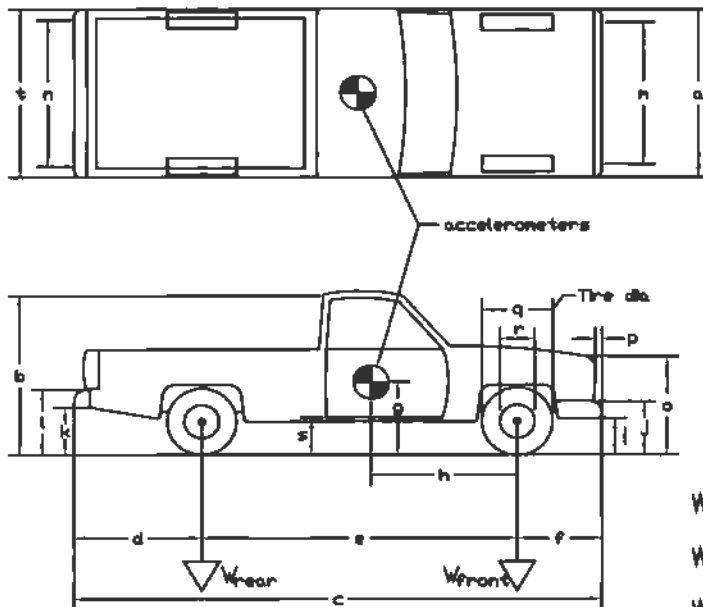
The front wheels of the test vehicle were aligned for camber, caster, and toe-in values of zero so that the vehicles would track properly along the guide cable. Two 5B flash bulbs were mounted on both the hood and roof of the vehicles to pinpoint the time of impact with the barrier system on the high-speed film. The flash bulbs were fired by a pressure tape switch mounted on the front face of the bumper. A remote controlled brake system was installed in the test vehicle so the vehicle could be brought safely to a stop after the test.



Figure 15. Test Vehicle, Test MWT-2

Date: 7/15/99 Test Number: MWT-2 Model: 2500
 Make: GMC Vehicle I.D.#: 1GDGC24K4PE506002
 Tire Size: 245/75 R16 Year: 1993 Odometer: 166353

*(All Measurements Refer to Impacting Side)



Vehicle Geometry - mm

a 1899 b 1842
 c 5544 d 1314
 e 3327 f 902
 g 738 h 1419
 i 495 j 654
 k 597 l 787
 m 1591 n 1626
 o 1016 p 102
 q 756 r 445
 s 495 t 1867

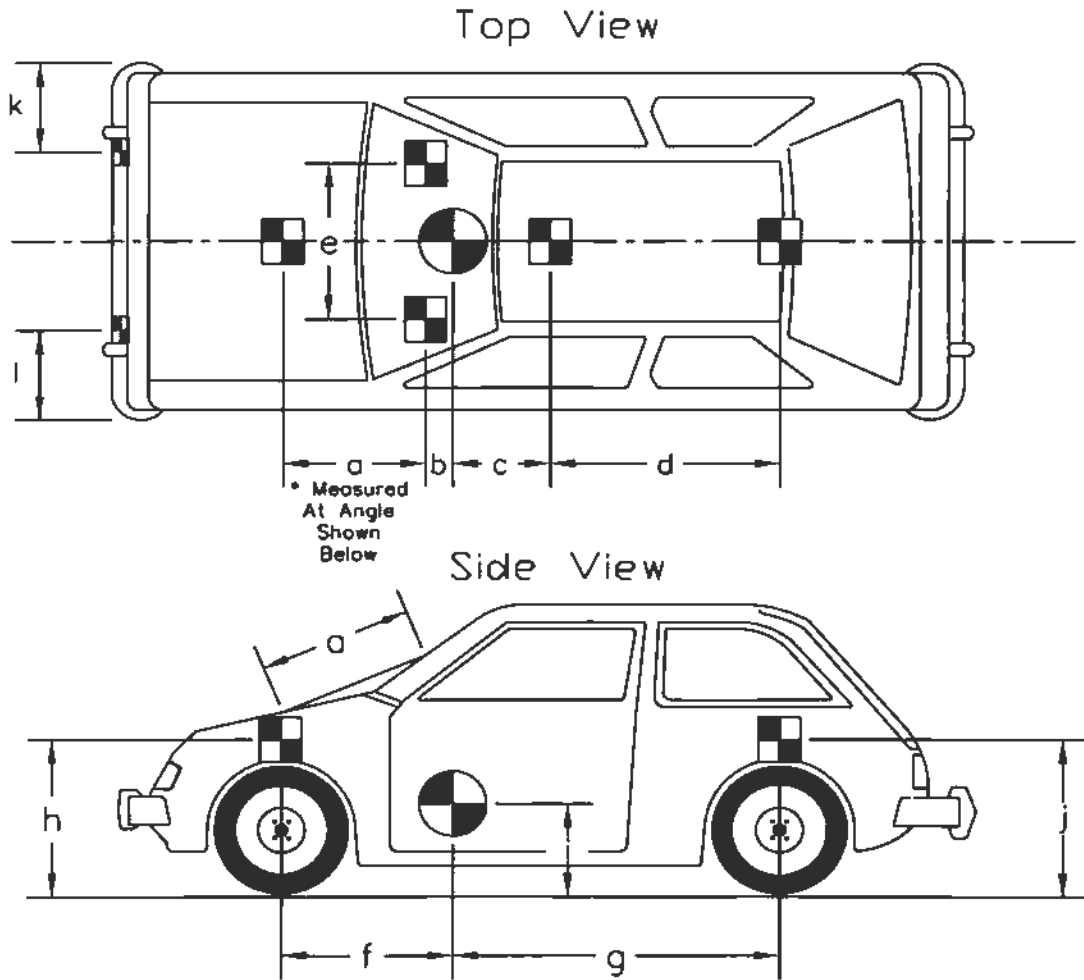
Wheel Center Height Front 368
 Wheel Center Height Rear 375
 Wheel Well Clearance (FR) 895
 Wheel Well Clearance (RR) 953

Engine Type 8 cyl. gas
 Engine Size 5.7 L 350 cid
 Transmission Type:
 Automatic or Manual
 FWD or RWD or 4WD

Weights - kg	Curb	Test Inertial	Gross Static
W _{front}	<u>1168</u>	<u>1159</u>	<u>1159</u>
W _{rear}	<u>863</u>	<u>863</u>	<u>863</u>
W _{total}	<u>2030</u>	<u>2022</u>	<u>2022</u>

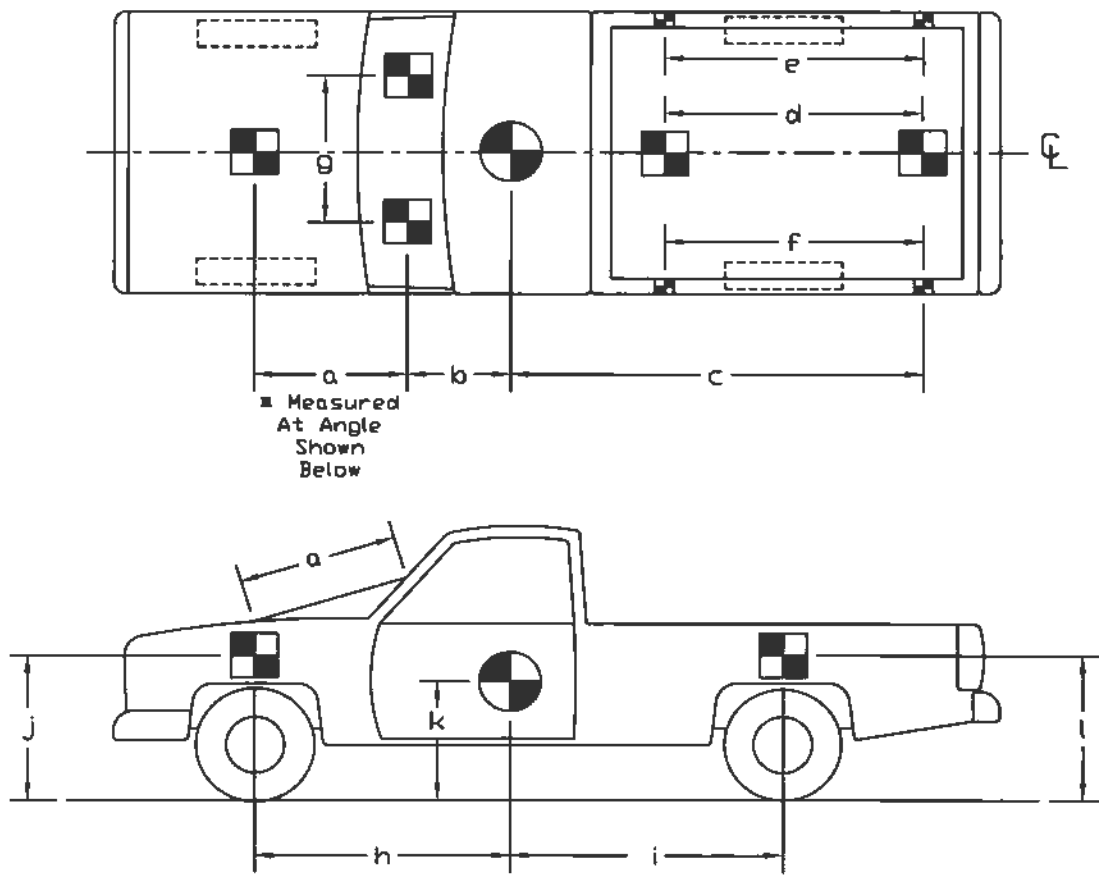
Note any damage prior to test: Right rear box dents

Figure 16. Vehicle Dimensions, Test MWT-2



TEST #:	MWT-1						
	TARGET GEOMETRY (mm)						
a	781	b	152	c	603	d	635
e	914	f	856	g	1430	h	686
		i	546	j	718		

Figure 17. Vehicle Target Locations, Test MWT-1



TEST #: <u>MWT-2</u>			
TARGET GEOMETRY (mm)			
a	<u>1099</u>	d	<u>1454</u>
b	<u>648</u>	e	<u>2153</u>
c	<u>2508</u>	f	<u>2153</u>
		g	<u>1060</u>
		h	<u>1419</u>
		i	<u>1905</u>
		j	<u>870</u>
		k	<u>738</u>
		l	<u>1054</u>

Figure 18. Vehicle Target Locations, Test MWT-2

5.4 Data Acquisition Systems

5.4.1 Accelerometers

One triaxial piezoresistive accelerometer system with a range of ± 200 G's was used to measure the acceleration in the longitudinal, lateral, and vertical directions at a sample rate of 10,000 Hz. The environmental shock and vibration sensor/recorder system, Model EDR-4M6, was developed by Instrumented Sensor Technology (IST) of Okemos, Michigan and includes three differential channels as well as three single-ended channels. The EDR-4 was configured with 6 Mb of RAM memory and a 1,500 Hz lowpass filter. Computer software, "DynaMax 1 (DM-1)" and "DADiSP" were used to digitize, analyze, and plot the accelerometer data.

A backup triaxial piezoresistive accelerometer system with a range of ± 200 G's was also used to measure the acceleration in the longitudinal, lateral, and vertical directions at a sample rate of 3,200 Hz. The environmental shock and vibration sensor/recorder system, Model EDR-3, was developed by Instrumented Sensor Technology (IST) of Okemos, Michigan. The EDR-3 was configured with 256 Kb of RAM memory and a 1,120 Hz lowpass filter. Computer software, "DynaMax 1 (DM-1)" and "DADiSP" were used to digitize, analyze, and plot the accelerometer data.

5.4.2 Rate Transducer

A Humphrey 3-axis rate transducer with a range of 360 deg/sec in each of the three directions (pitch, roll, and yaw) was used to measure the rates of motion of the test vehicle. The rate transducer was rigidly attached to the vehicles near the center of gravity of the test vehicle. Rate transducer signals, excited by a 28 volt DC power source, were received through the three single-ended channels located externally on the EDR-4M6 and stored in the internal memory. The raw data measurements were then downloaded for analysis and plotting. Computer software, "DynaMax 1

(DM-1)" and "DADiSP" were used to digitize, analyze, and plot the rate transducer data.

5.4.3 High-Speed Photography

For test MWT-1, five high-speed 16-mm Red Lake Locam cameras, with operating speeds of approximately 500 frames/sec, were used to film the crash test. A Locam, with a wide-angle 12.5-mm lens, was placed above the test installation to provide a field of view perpendicular to the ground. A Locam, with a zoom lens, a SVHS video camera, and a 35-mm still camera were placed downstream from the impact point and had a field of view parallel to the barrier. A Locam, with a zoom lens, and a SVHS video camera were placed on the traffic side of the barrier and had a field of view perpendicular to the barrier. A Locam, with a 12.5-mm lens, was placed upstream and behind the barrier. A Locam and a SVHS video camera were placed downstream and behind the barrier. A schematic of all nine camera locations for test MWT-1 is shown in Figure 19.

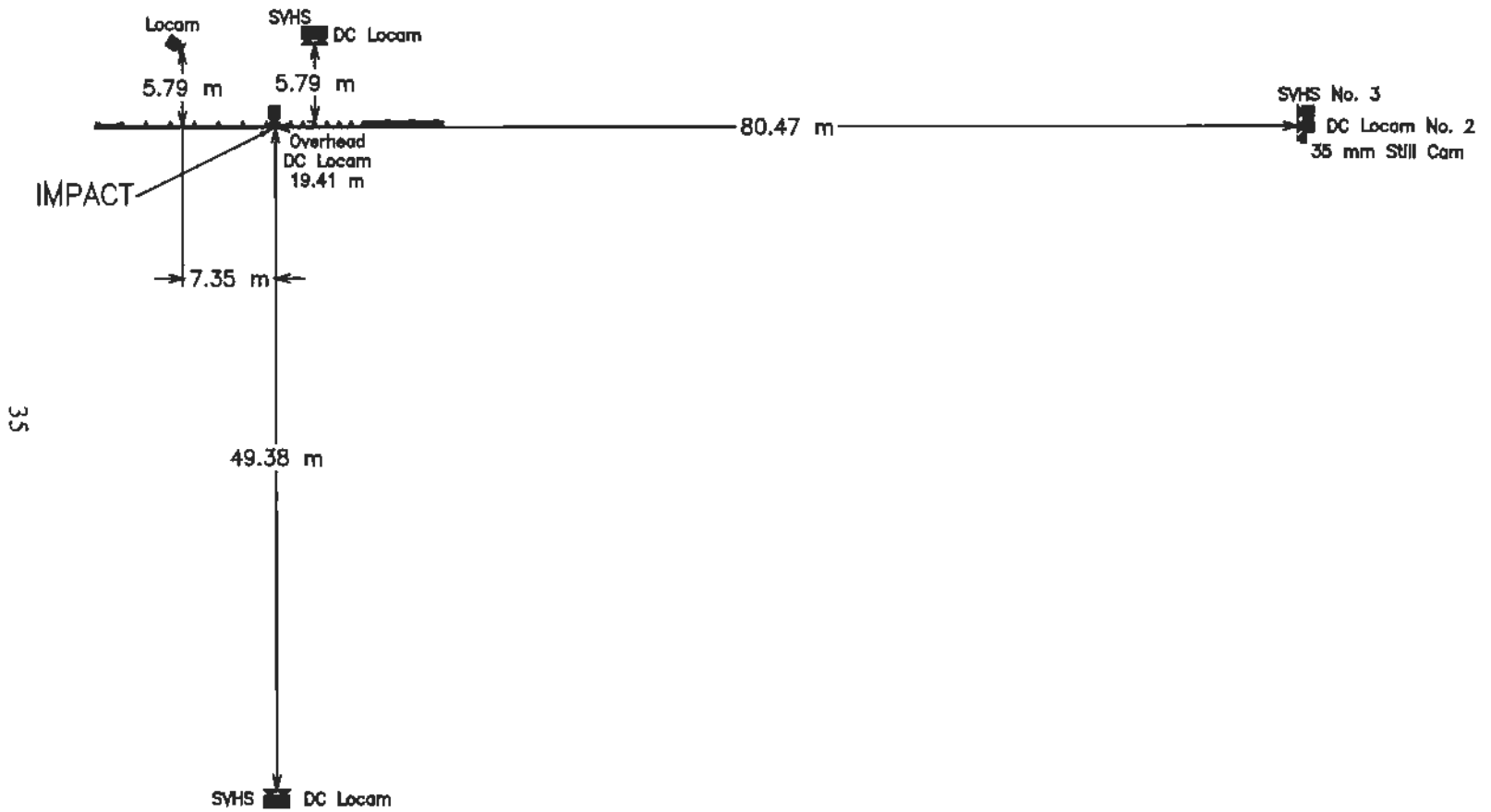
For test MWT-2, five high-speed 16-mm Red Lake Locam cameras, with operating speeds of approximately 500 frames/sec, were used to film the crash test. A Locam, with a wide-angle 12.5-mm lens, was placed above the test installation to provide a field of view perpendicular to the ground. A Locam, with a zoom lens, a SVHS video camera, and a 35-mm still camera were placed downstream from the impact point and had a field of view parallel to the barrier. A Locam, with a zoom lens, and a SVHS video camera were placed on the traffic side of the barrier and had a field of view perpendicular to the barrier. A Locam, with a 12.5-mm lens, and a SVHS video camera were placed downstream and behind the barrier. Another Locam was placed downstream and behind the barrier but closer to the system. A schematic of all nine camera locations for test MWT-2 is shown in Figure 20.

The film was analyzed using the Vanguard Motion Analyzer. Actual camera speed and

camera divergence factors were considered in the analysis of the high-speed film.

5.4.4 Pressure Tape Switches

For both crash tests, five pressure-activated tape switches, spaced at 2-m intervals, were used to determine the speed of the vehicle before impact. Each tape switch fired a strobe light which sent an electronic timing signal to the data acquisition system as the left front tire of the test vehicle passed over it. Test vehicle speeds were determined from electronic timing mark data recorded on "Test Point" software. Strobe lights and high-speed film analysis are used only as a backup in the event that vehicle speeds cannot be determined from the electronic data.



35

Figure 19. Location of High-Speed Cameras, Test MWT-1

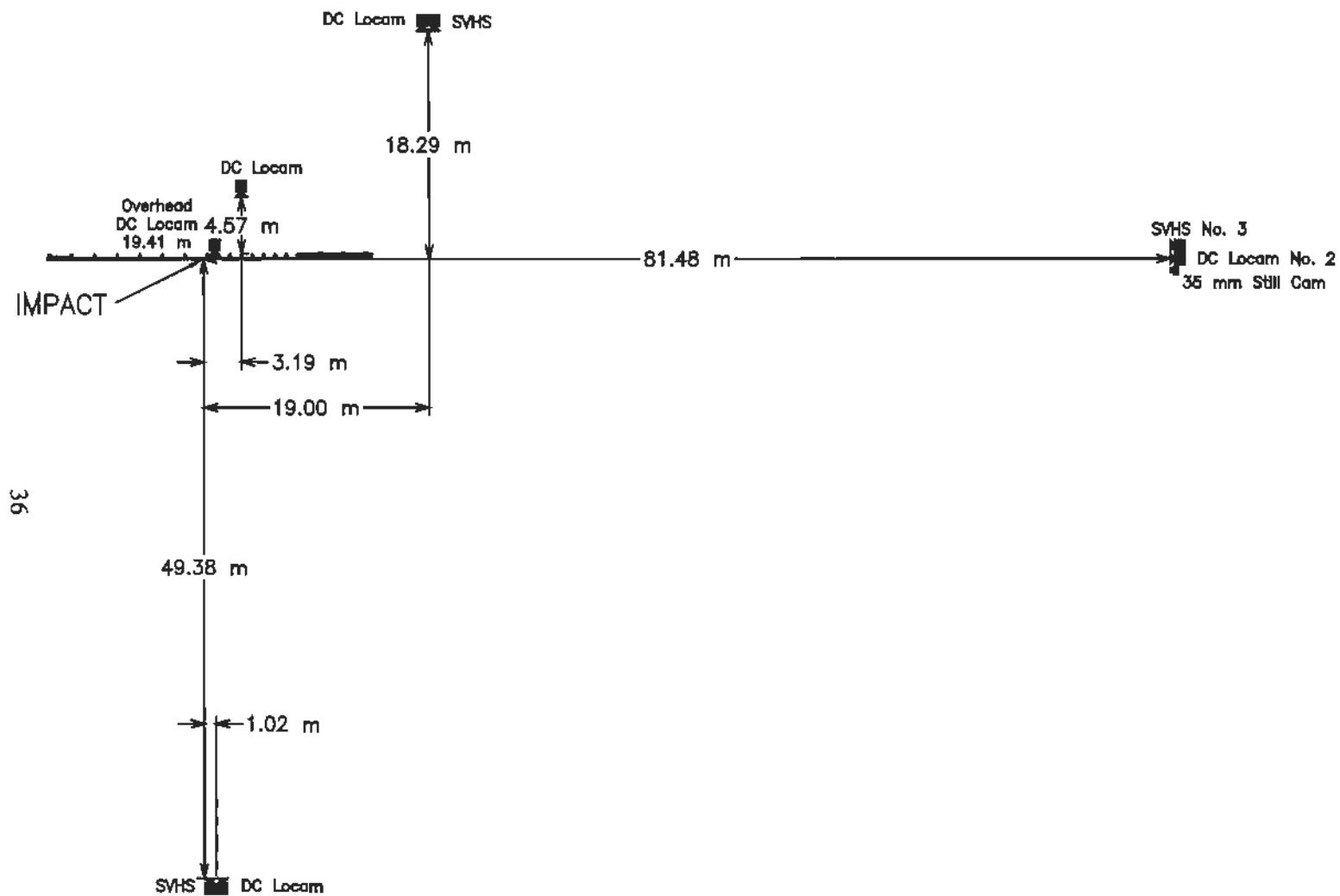


Figure 20. Location of High-Speed Cameras, Test MWT-2

6 COMPUTER SIMULATION

6.1 Background

Computer simulation modeling with BARRIER VII (10) was performed to analyze and predict the dynamic performance of a W-beam to thrie beam transition section used in conjunction with an approach guardrail transition design. The simulations were conducted modeling: (1) a 2000-kg pickup truck impacting at a speed of 100.0 km/hr and at an angle of 25 degrees; and (2) an 820-kg small car impacting at a speed of 100.0 km/hr and at an angle of 20 degrees. Typical computer simulation input data files for both impact scenarios are shown in Appendix A.

Computer simulation was also used to determine the critical impact point (CIP) for the W-beam to thrie beam transition section. For the pickup truck impact, the CIP was based upon the impact condition which produced the greatest potential for wheel-assembly snagging on the steel post located on the downstream end of the W-beam to thrie beam transition section. For the small car impact, the CIP was based on the impact condition which produced the greatest potential for vehicle wedging underneath the tapered rail. This condition was believed to occur when the dynamic lateral rail deflections were maximized at the midpoint of the W-beam to thrie beam transition section.

6.2 BARRIER VII Results

Several computer simulation runs were performed on the barrier system with each vehicle type. For the pickup truck impact, the CIP was determined to occur with an impact between post nos. 9 and 10 or 330-mm upstream from the centerline of post no. 9. For the small car impact, the CIP was determined to occur with an impact between post nos. 8 and 9 or 1,219-mm upstream from the centerline of post no. 8.

7 CRASH TEST NO. 1

7.1 Test MWT-1

The 896-kg small car impacted the guardrail system upstream from the W-beam to thrie beam transition element at a speed of 99.5 km/hr and an angle of 25.7 degrees. A summary of the test results and the sequential photographs are shown in Figure 21. Additional sequential photographs are shown in Figure 22. Documentary photographs of the crash test are shown in Figures 23 through 25.

7.2 Test Description

Initial impact occurred between post nos. 8 and 9 or 1,219-mm upstream from the center of post no. 8, as shown in Figure 26. At 0.040 sec after impact, the left-front corner of the vehicle was at post no. 8, and the hood began to bulge upward and separate from the fenders. At 0.052 sec, the left-front tire only rubbed across the face of post no. 8. At this same time, the left-front fender crushed inward toward the engine compartment, and the top of the left-side door separated from the top of the vehicle. At 0.081 sec, the left-front corner of the vehicle was at post no. 7. At 0.098 sec, the left-front tire wedged under the W-beam to thrie beam transition section, and the tire impacted the bottom of the wooden blockout at post no. 7 and snagged on post no. 7. At this same time, the left-side window shattered. At 0.113 sec, the left-front corner of the vehicle was at post no. 6. At 0.126 sec, the deformed left-front tire, still wedged under the rail, was at the midpoint between post nos. 6 and 7. At this same time, the front of the vehicle was downstream from post no. 6 and with the dummy's head protruding out of the left-door's shattered window. At 0.149 sec, the left rear of the vehicle contacted the guardrail with the rear bumper slightly upstream of post no. 8. At this same time, the shattered glass from the left-side door was flying away from the vehicle. At 0.150 sec, the

left-front tire twisted the wooden blockout at post no. 6 and contacted post no. 6. At this same time, the rear end of the vehicle impacted the rail near post no. 8, and the left-rear tire became slightly airborne. At 0.153 sec, the front of the vehicle was at post no. 5. At 0.161 sec after impact, the vehicle became parallel to the barrier with a velocity of 69.8 km/hr, and the front of the vehicle began to separate from the guardrail. At 0.200 sec, the left-rear tire was at post no. 7, and the wooden blockout at post no. 6 twisted and split. At 0.203 sec, the front of the vehicle was at post no. 4 but not in contact with the rail. At 0.212 sec, the right-rear tire became airborne. At 0.25 sec, the vehicle reached its maximum yaw angle of 26.9 degrees. At 0.258 sec, the left-rear tire was back on the ground. At 0.264 sec after impact, the vehicle, with its rear bumper at post no. 6, exited the guardrail at an angle of 4.3 degrees and a speed of 65.6 km/hr. At 0.366 sec, the rear of the vehicle, not in contact with the rail, was at post no. 4 and yawed counter-clockwise (CCW) away from the guardrail. At 0.38 sec, the vehicle reached its maximum roll angle of 6.1 degrees, and at 0.8 sec, the vehicle reached its maximum pitch angle of 11 degrees. The vehicle's post-impact trajectory is shown in Figures 21 and 27. The vehicle came to rest 43.28 m downstream from impact and 8.81 m away from the traffic-side face of the rail, as shown in Figures 21 and 27.

7.3 Barrier Damage

Damage to the barrier was minimal, as shown in Figures 28 through 32. Barrier damage consisted mostly of deformed W-beam, contact marks on a guardrail sections, deformed guardrail posts, and damaged spacer blocks. The W-beam to thrie beam transition element damage consisted of moderate deformation and flattening of the lower corrugation. Contact marks were found on the W-beam and W-beam to thrie beam section between post nos. 6 and 9. Black marks were found along the bottom corrugation and green and red marks were found on the top and middle

corrugations of the rail between post nos. 6 and 9. The top of the rail buckled 25-mm upstream of post no. 6. The bottom of the rail was flattened against the wood blockout at post no. 7.

During the impact event, damage and deformations were observed at several post locations and consisted of permanent post deformations, contact marks, and damaged wooden blockouts. Post nos. 5 through 8 deflected backwards. Post no. 7 also was twisted. Black contact marks were found on the front faces of post nos. 6 through 8 and the wood blockouts of post nos. 7 and 8. The wood blockouts at post nos. 6, 9, and 10 were cracked. The wood blockout at post no. 6 also was split. No significant post or guardrail damage occurred upstream of post no. 10 nor downstream of post no. 4.

The permanent set of the guardrail and posts is shown in Figure 32. The maximum lateral permanent set rail and post deflections were approximately 108 mm at the center line of post no. 8 and 114 mm at post no. 8, respectively, as measured in the field. The maximum lateral dynamic rail and post deflections were 220 mm at the centerline of post nos. 7 and 8, as determined from the high-speed film analysis.

7.4 Vehicle Damage

Exterior and interior vehicle damage was moderate, as shown in Figures 33 through 35. Most of the vehicle damage occurred near the left-front corner of the vehicle, as shown in Figure 34. The left-front corner was crushed inward toward the engine. The major left-front wheel components, such as the lower A-frame, the tie rod end, the brake line, and the shock attachment, disengaged. Major damage occurred to the left-front tire rim, and the tire was slashed. The vehicle's left side encountered contact marks and deformations due to the vehicle/rail interlock. The engine hood was shifted to the right, and the grill disengaged from the front mounts. The plastic, front-bumper cover

was also deformed. The left-door's window was shattered. The top of the left door was ajar, and the lower portion of the door was deformed inward. A longitudinal buckling point was found on the left side of the roof, 660 mm from the A-pillar. The maximum occupant compartment deformation occurred near the lower-left corner of floorboard as the sheet metal was pushed inward 104 mm. The right side and rear remained undamaged.

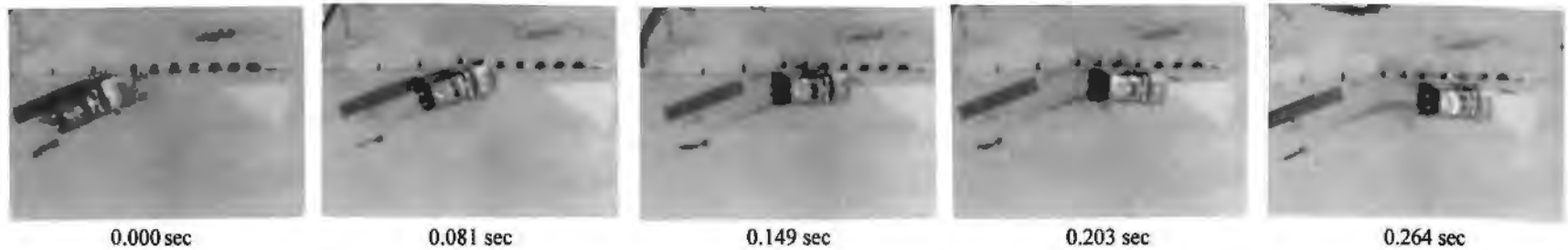
7.5 Occupant Risk Values

The longitudinal and lateral occupant impact velocities were determined to be 6.21 m/sec and 7.00 m/sec, respectively. The maximum 0.010-sec average occupant ridedown decelerations in the longitudinal and lateral directions were 10.67 g's and 9.80 g's, respectively. It is noted that the occupant impact velocities (OIV) and occupant ridedown decelerations (ORD) were within the suggested limits provided in NCHRP Report No. 350. The results of the occupant risk, as determined from the accelcrometer data, are summarized in Figure 21. Results are shown graphically in Appendix B. The results from the rate transducer are shown graphically in Appendix C.

7.6 Discussion

The analysis of the test results for test MWT-1 showed that the barrier satisfactorily contained and redirected the vehicle with controlled lateral displacements of the guardrail. Detached elements, fragments, or other debris from the test article did not penetrate or show potential for penetrating the occupant compartment, or present undue hazard to other traffic. Deformation of, or intrusion into, the occupant compartment that could have caused serious injury did not occur. The vehicle remained upright during and after collision. Vehicle roll, pitch, and yaw angular displacements were noted, but they were deemed acceptable because they did not adversely influence

occupant risk safety criteria nor cause rollover. After collision, the vehicle's trajectory intruded slightly into adjacent traffic lanes but was determined to be acceptable. In addition, the vehicle's exit angle was less than 60 percent of the impact angle. Therefore, test MWT-1 conducted on the W-beam to three beam transition element was determined to be acceptable according to the NCHRP Report No. 350 criteria.



- Test Number MWT-1
- Date 7/8/99
- Appurtenance W-beam to Thrie Beam
Transition Element
- Total Length 26.67 m
- Steel W-Beam to Thrie Beam Transition
 - Thickness 2.66 mm
 - Top Mounting Height 803 mm
- Steel Posts
 - Post Nos. 1 - 5 W152x22.3 by 2,135-mm long
 - Post Nos. 6 - 8 W152x13.4 by 1,980-mm long
 - Post Nos. 9 - 14 W152x13.4 by 1,830-mm long
- Wood Spacer Blocks
 - Post No. 1 203 mm x 203 mm by 380-mm long
 - Post Nos. 2 - 5 203 mm x 203 mm by 480-mm long
 - Post No. 6 152 mm x 203 mm by 554-mm long
 - Post No. 7 152 mm x 203 mm by 483-mm long
 - Post No. 8 - 14 152 mm x 203 mm by 360-mm long
- Soil Type Grading B - AASHTO M 147-65 (1990)
- Vehicle Model 1993 Ford Festiva
 - Curb 814 kg
 - Test Inertial 821 kg
 - Gross Static 896 kg
- Vehicle Speed
 - Impact 99.5 km/hr
 - Exit 18.22 km/hr
- Vehicle Angle
 - Impact 25.7 degrees
 - Exit 4.29 degrees
- Vehicle Snagging Minor wheel contact with
post nos. 6 and 7
- Vehicle Pocketing None
- Vehicle Stability Satisfactory
- Occupant Ridedown Deceleration (10 msec avg.)
 - Longitudinal 10.67 < 20 G's
 - Lateral (not required) 9.80
- Occupant Impact Velocity
 - Longitudinal 6.21 < 12 m/s
 - Lateral (not required) 7.00
- Vehicle Damage Moderate
 - TAD¹¹ 11-LFQ-4
 - SAE¹² 11-LFEW3
- Vehicle Stopping Distance 43.28 m downstream
8.81 m traffic-side face
- Barrier Damage Minimal
- Maximum Deflections
 - Permanent Set 108 mm
 - Dynamic 220 mm

Figure 21. Summary of Test Results and Sequential Photographs, Test MWT-1



0.000 sec



0.010 sec



0.040 sec



0.070 sec



0.096 sec



0.102 sec



0.000 sec



0.038 sec



0.098 sec



0.126 sec



0.150 sec



0.200 sec

Figure 22. Additional Sequential Photographs, Test MWT-1



45

Figure 23. Documentary Photographs, Test MWT-1



46

Figure 24. Documentary Photographs, Test MWT-1



47



Figure 25. Documentary Photographs, Test MWT-1



Figure 26. Impact Location, Test MWT-1



Figure 27. Final Vehicle Position, Test MWT-1



Figure 28. W-beam to Thrie Beam Transition Damage, Test MWT-1



Figure 29. W-beam to Thrie Beam Transition Damage, Test MWT-1



Figure 30. Post Nos. 7 and 8 Damage, Test MWT-1



Figure 31. Wooden Blockout Damage, Test MWT-1

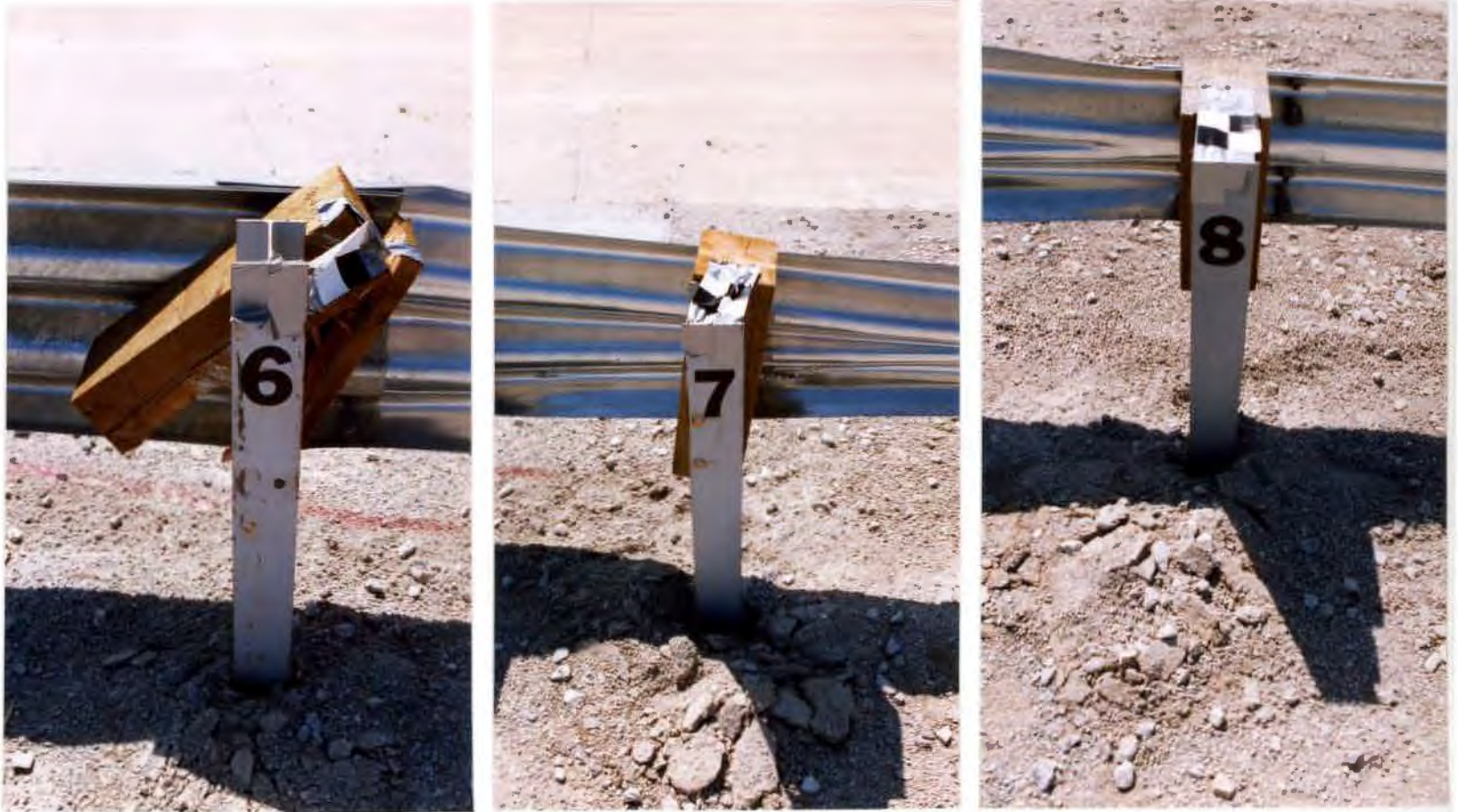


Figure 32. Permanent Set Deflections, Test MWT-1



Figure 33. Vehicle Damage, Test MWT-1



Figure 34. Vehicle Damage, Test MWT-1



Figure 35. Occupant Compartment Deformations, Test MWT-1

8 CRASH TEST NO. 2

8.1 Test MWT-2

The 2,022-kg pickup truck impacted the guardrail system upstream from the W-beam to thrie beam transition element at a speed of 98.3 km/hr and an angle of 25.3 degrees. A summary of the test results and the sequential photographs are shown in Figure 36. Additional sequential photographs are shown in Figures 37 and 38. Documentary photographs of the crash test are shown in Figures 39 through 41.

8.2 Test Description

Initial impact occurred between post nos. 9 and 10 or 330-mm upstream from the center of post no. 9, as shown in Figure 42. At 0.040 sec after impact, the left-front corner of the vehicle was at the midspan between post nos. 8 and 9. At this same time, post no. 9 was observed to be pushed backward and away from its original position. At 0.056 sec, post no. 8 began to twist CCW, and the left-front side of the bumper and lower fender crushed inward. At this same time, the left-front corner of the engine hood and upper edge of the fender became separated. At 0.080 sec, the left-front corner of the vehicle was at post no. 8, and the left-front tire had turned sideways. At this same time, post no. 7 had not moved, although significant twist about its longitudinal axis was observed in the rail between post nos. 7 and 8. At 0.094 sec, post no. 7 began to deflect backward and twist about its vertical axis. At 0.102 sec, the deformed left-front tire snagged on the bottom of post no. 8 which had deflected, causing the tire to turn sharply to the left. However, the tire was not captured under the rail. At 0.113 sec, post no. 6 began to deflect away from its original position. At 0.117 sec, the rail upstream of post no. 6 kinked across the full depth. At 0.124 sec, significant vehicle pocketing in the rail upstream of post no. 7 was observed. At this same time, post no. 7 was

deflected backward and downstream in response to the vehicle pocketing. At 0.129 sec, the left-front corner of the vehicle extended over post no. 7, and the middle front of the vehicle was ready to impact post no. 6. At this same time, there was very little, if any, redirection of the vehicle, and the top of the left-side door separated from the top of the cab. At 0.135 sec, post no. 6 twisted and deflected backward. At this same time, the wooden blockout at post no. 8 splintered due to the contact between the tire and suspension and the bottom of the blockout. At 0.151 sec, the vehicle was on post no.6. At this same time, extensive damage to the vehicle's front bumper and left side was observed and occurred as the vehicle contacted the guardrail upstream from post no. 6. Slightly after this time, the vehicle redirected appreciably. At 0.165 sec, the top of the rail tore slightly upstream of post no. 6 with the deformed left-front corner of the vehicle positioned at this point. At 0.185 sec, the truck traveled over the deformed post no. 5. After this time, the vehicle rolled CCW away from the rail. At 0.189 sec, post no. 7 was pushed toward the ground. At this same time, the right-front tire became airborne as the front of the vehicle began to rise into the air. At 0.248 sec, the left-front wheel began to ride up on the system as the wooden blockout at post no. 5 rotated. At 0.251 sec, the front of the vehicle extended over post no. 4. At 0.261 sec, the front bumper lost contact with the system. At 0.316 sec, the left-front tire was on top of the system with the vehicle rolling CCW away from the rail. At 0.340 sec, the left-front tire was above the system after climbing and vaulting away from the system at post no. 5. At 0.346 sec, the front of the vehicle extended over post no. 3. At 0.448 sec, the front of the vehicle extended over post no. 2 as the vehicle encountered significant CCW roll. At this point, the left-rear tire and the rear end of the vehicle had not touched the rail. At 0.480 sec, the front end of the vehicle was airborne as well as the left-rear tire being higher than the top of the rail. At 0.524 sec, the vehicle was pivoting about the right-rear tire, which

was the only tire in contact with the ground. At 0.661 sec, the left-rear tire impacted the rail near post no. 5. At 0.854 sec, the left-front corner was at its highest point in the air, and the vehicle was positioned well away from the rail. At this same time, the right corner of the rear bumper was in contact with the ground. At 1.266 sec, the vehicle's right side landed on the ground. At 1.29 sec, the vehicle reached its maximum pitch angle of 61 degrees. The vehicle's post-impact trajectory is shown in Figures 36 and 43. The vehicle came to rest 11.07 m downstream from impact and 3.05 m away from the traffic-side face of the rail, as shown in Figures 36 and 43.

8.3 Barrier Damage

Damage to the barrier was moderate, as shown in Figures 44 through 50. Barrier damage consisted mostly of deformed guardrail including W-beam, W-beam to thrie beam transition, and thrie beam, contact marks on a guardrail, deformed guardrail posts, and damaged spacer blocks. The W-beam damage consisted of moderate deformation and flattening of the lower portion of the impacted section between post nos. 8 and 9. The W-beam to thrie beam transition damage consisted of moderate deformation and flattening of the impacted section of transition between post nos. 6 and 8. The thrie beam damage consisted of moderate deformation and flattening of the impacted section of rail between post nos. 4 and 6. The W-beam to thrie beam transition element ripped at the guardrail splice located on the upstream side of post no. 6, as shown in Figure 45. Contact marks were found on the guardrail between post nos. 4 and 10.

During the impact event, damage and deformations were observed at several post locations and consisted of permanent post deformations, contact marks, and damaged wooden blockouts. Post nos. 10 through 14 were twisted and the bolts pulled through the bolt holes in the guardrail causing slot damage. Post no. 9 was not contacted but twisted and rotated backward. Post no. 8 was

contacted on the front edge and nearly flattened. Post no. 7 was not contacted, but was rotated and deformed to the ground. Post no. 6 was not contacted, but was twisted and flattened. Post nos. 2 through 5 were not contacted, but moved slightly with soil failure. The wood blockout at post no. 5 split down the blockout's length at the traffic-side quarter-point. No significant post or guardrail damage occurred downstream of post no. 1.

The permanent set of the guardrail and posts is shown in Figures 47 through 49. The cable anchorage system encountered slight permanent deformation due to the tensile loads transmitted through the guardrail, as shown in Figure 50. The maximum lateral dynamic rail and post deflections were 806 mm at the centerline of post nos. 4 through 6 and 806 mm at post no. 6, respectively, as determined from the high-speed film analysis.

8.4 Vehicle Damage

Exterior and interior vehicle damage was extensive and occurred at several body locations, as shown in Figures 51 through 53. Most of the vehicle damage occurred to the left-front corner of the vehicle. Severe deformation and damaged occurred to the left-front frame and bracket, the left-front wheel and suspension, and the front bumper. All of the major left-front wheel linkages, including the tie rod, the ball joint, and the sway bar, disengaged. The engine and transmission mounts also disengaged. Deformation occurred to the drive shaft. The left-front steel rim encountered major damage. The floorboard's center hump buckled toward the occupant compartment's rear wall. The firewall of the occupant compartment crushed inward under the brake pedal. All the window glass remained undamaged.

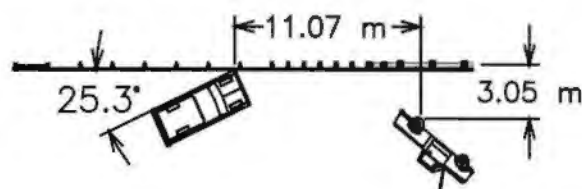
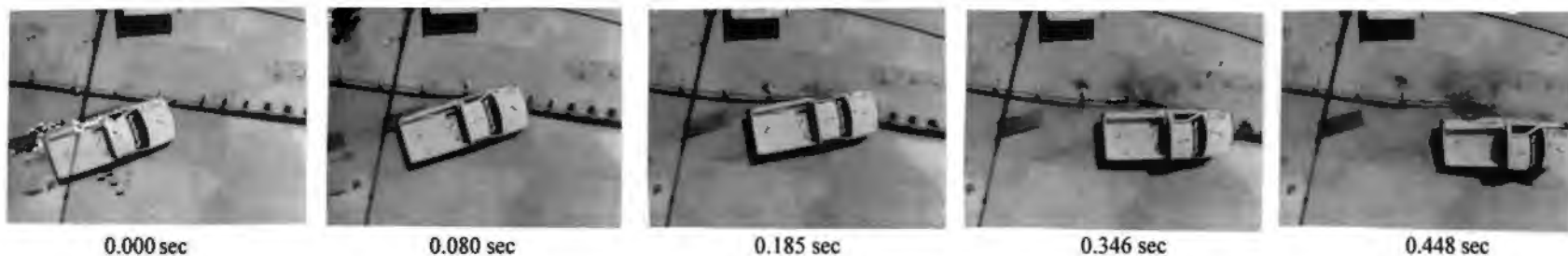
8.5 Occupant Risk Values

The longitudinal and lateral occupant impact velocities were determined to be 8.17 m/sec and

4.97 m/sec, respectively. The maximum 0.010-sec average occupant ridedown decelerations in the longitudinal and lateral directions were 13.49 g's and 9.05 g's, respectively. It is noted that the occupant impact velocities (OIV) and occupant ridedown decelerations (ORD) were within the suggested limits provided in NCHRP Report No. 350. The results of the occupant risk, as determined from the accelerometer data, are summarized in Figure 36. Results are shown graphically in Appendix D. The results from the rate transducer are shown graphically in Appendix E.

8.6 Discussion

The analysis of the test results for test MWT-2 showed that the barrier contained but did not adequately redirect the vehicle since the vehicle did not remain upright after collision with the W-beam to thrie beam transition element. Detached elements, fragments, or other debris from the test article did not penetrate or show potential for penetrating the occupant compartment, or present undue hazard to other traffic. Major deformations to the occupant compartment were evident. After collision, the vehicle's trajectory intruded into adjacent traffic lanes. Therefore, test MWT-2 conducted on the W-beam to thrie beam transition element was determined to be unacceptable according to the NCHRP Report No. 350 criteria.



63

- Test Number MWT-2
- Date 7/15/99
- Appurtenance W-beam to Thrie Beam Transition Element
- Total Length 26.67 m
- Steel W-Beam to Thrie Beam Transition
 - Thickness 2.66 mm
 - Top Mounting Height 803 mm
- Steel Posts
 - Post Nos. 1 - 5 W152x22.3 by 2,135-mm long
 - Post Nos. 6 - 8 W152x13.4 by 1,980-mm long
 - Post Nos. 9 - 14 W152x13.4 by 1,830-mm long
- Wood Spacer Blocks
 - Post No. 1 203 mm x 203 mm by 380-mm long
 - Post Nos. 2 - 5 203 mm x 203 mm by 480-mm long
 - Post No. 6 152 mm x 203 mm by 554-mm long
 - Post No. 7 152 mm x 203 mm by 483-mm long
 - Post No. 8 - 14 152 mm x 203 mm by 360-mm long
- Soil Type Grading B - AASHTO M 147-65 (1990)
- Vehicle Model 1993 GMC 2500 ¼-ton pickup
 - Curb 2,030 kg
 - Test Inertial 2,022 kg
 - Gross Static 2,022 kg

- Vehicle Speed
 - Impact 98.3 km/hr
 - Exit NA
- Vehicle Angle
 - Impact 25.3 degrees
 - Exit NA
- Vehicle Snagging Snagging on post no. 8
- Vehicle Pocketing Moderate
- Vehicle Stability Vehicle rollover
- Occupant Ridedown Deceleration (10 msec avg.)
 - Longitudinal 13.49 < 20 G's
 - Lateral (not required) 9.05
- Occupant Impact Velocity
 - Longitudinal 8.17 < 12 m/s
 - Lateral (not required) 4.97
- Vehicle Damage Extensive
 - TAD¹¹ NA
 - SAE¹² NA
- Vehicle Stopping Distance 11.07 m downstream
3.05 m traffic-side face
- Barrier Damage Moderate
- Maximum Deflections
 - Permanent Set NA
 - Dynamic 806 mm

Figure 36. Summary of Test Results and Sequential Photographs, Test MWT-2



0.000 sec



0.094 sec



0.113 sec



0.189 sec



0.261 sec



0.316 sec



0.374 sec



0.524 sec



0.854 sec



1.266 sec

Figure 37. Additional Sequential Photographs, Test MWT-2



0.000 sec



0.102 sec



0.124 sec



0.190 sec



0.248 sec



0.340 sec



0.000 sec



0.056 sec



0.093 sec



0.135 sec



0.165 sec



0.192 sec

Figure 38. Additional Sequential Photographs, Test MWT-2



Figure 39. Documentary Photographs, Test MWT-2



Figure 40. Documentary Photographs, Test MWT-2



Figure 41. Documentary Photographs, Test MWT-2



69



Figure 42. Impact Location, Test MWT-2



Figure 43. Final Vehicle Position, Test MWT-2



Figure 44. W-beam to Thrie Beam Transition Damage, Test MWT-2

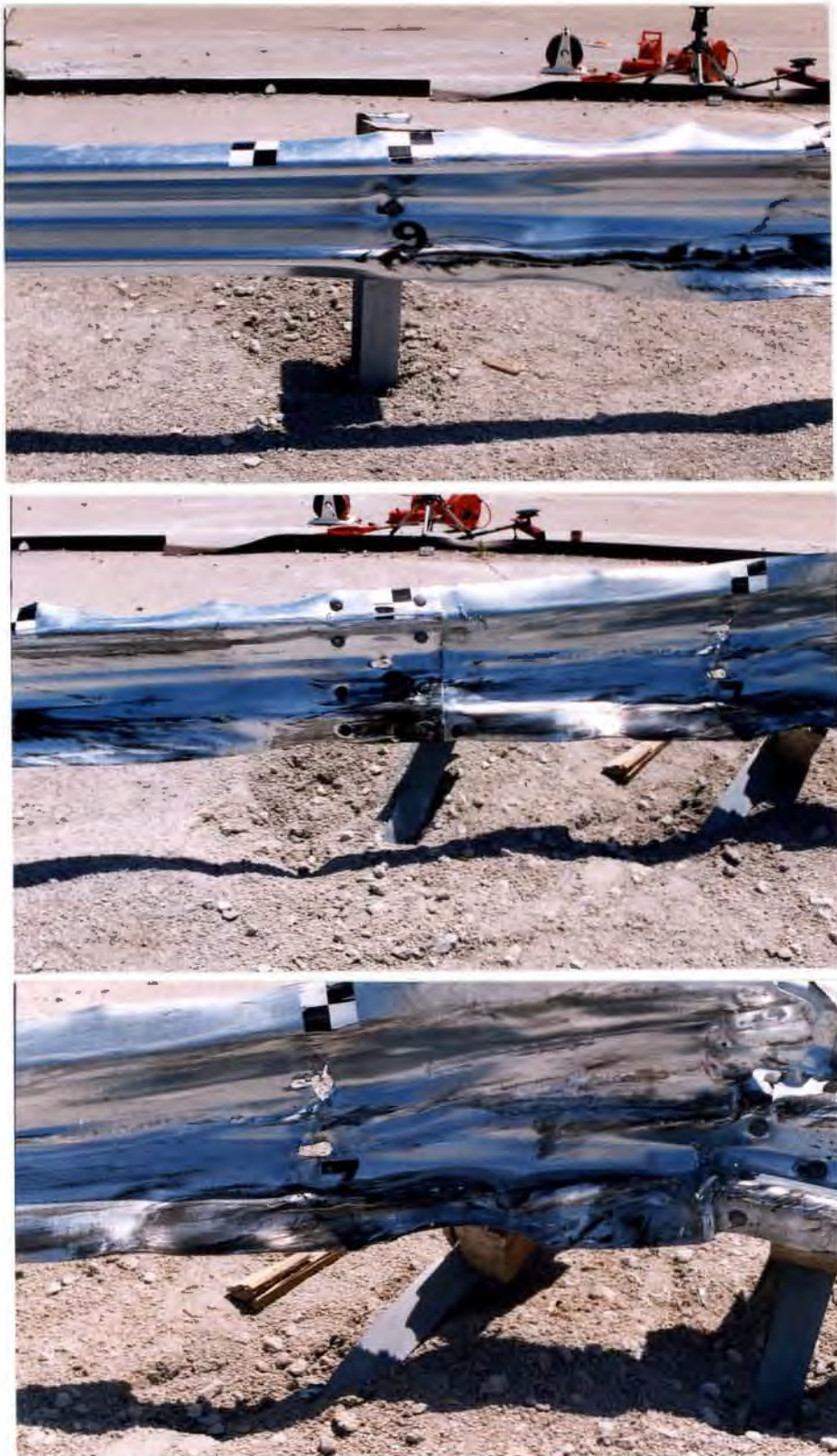


Figure 45. W-beam to Thrie Beam Transition Damage, Test MWT-2



Figure 46. W-beam to Thrie Beam Transition Damage, Test MWT-2



Figure 47. Post Nos. 4 and 5 Damage, Test MWT-2



Figure 48. Post No. 6 and 7 Damage, Test MWT-2

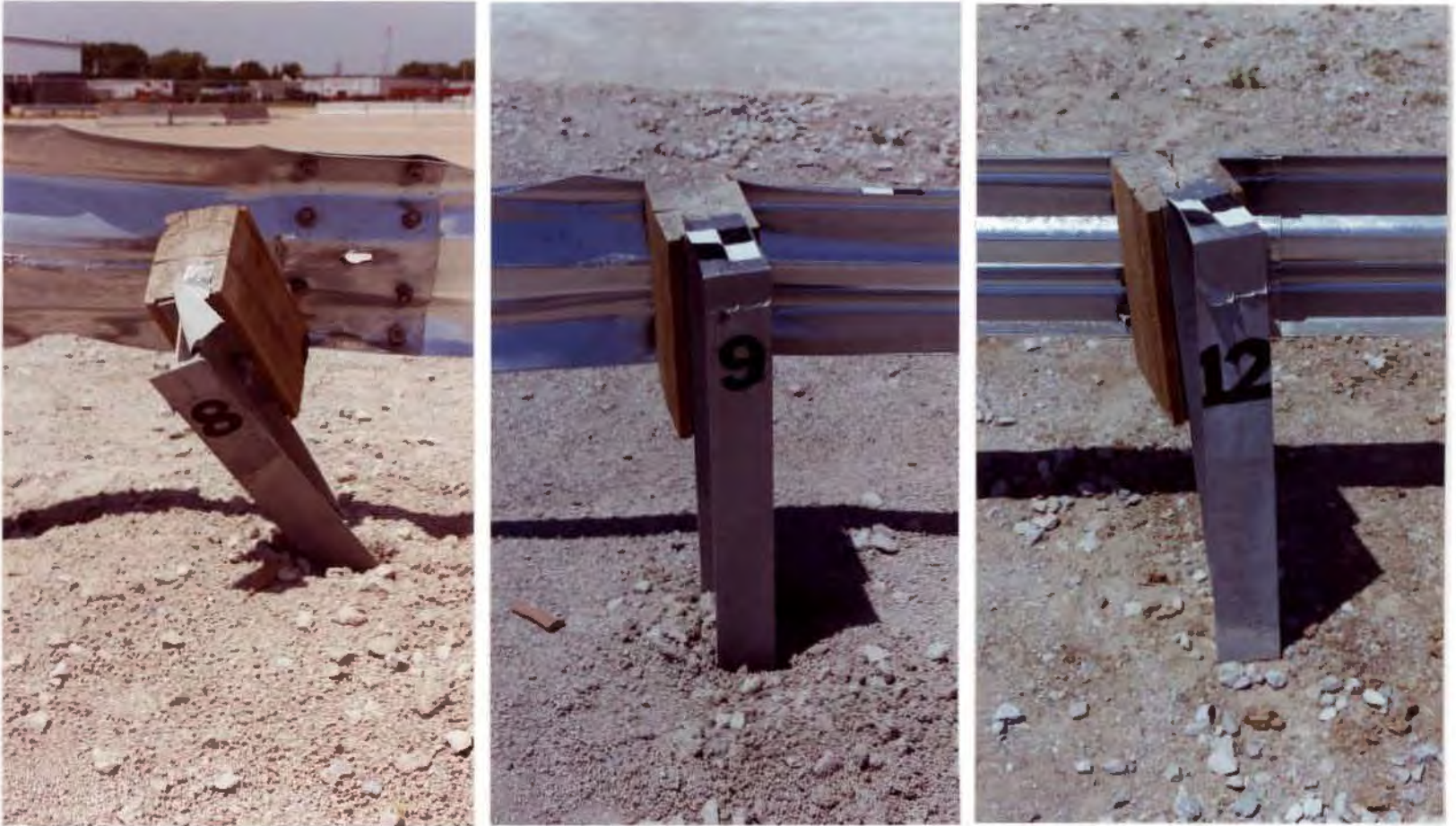


Figure 49. Post Nos. 8, 9, and 12 Damage, Test MWT-2



Figure 50. Permanent Set Deflections, Test MWT-2



Figure 51. Vehicle Damage, Test MWT-2



Figure 52. Vehicle Damage, Test MWT-2

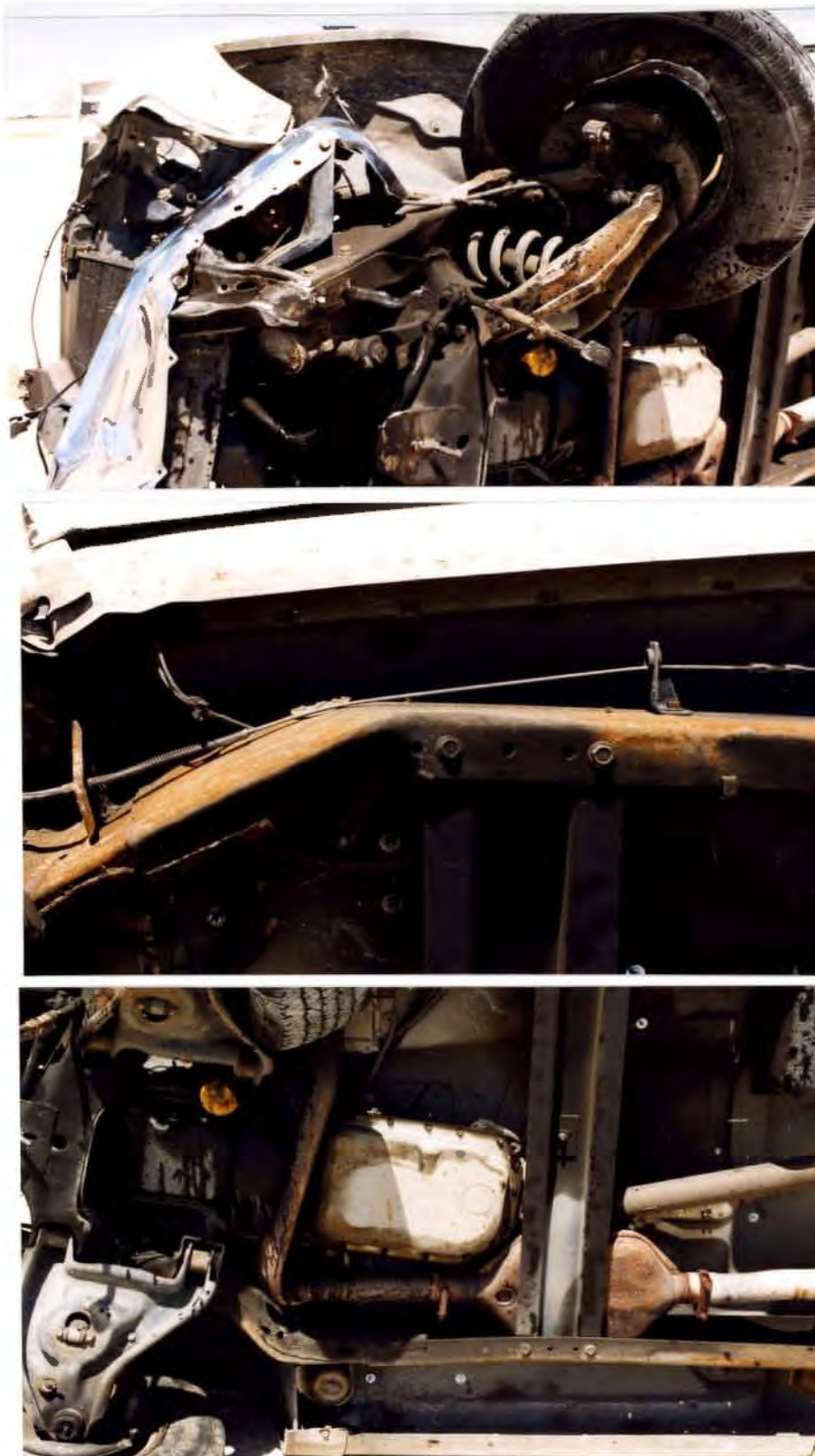


Figure 53. Under-Carriage Vehicle Damage, Test MWT-2

9 SUMMARY AND CONCLUSIONS

A W-beam to thrie beam transition element was constructed in conjunction with a strong-post W-beam guardrail and an approach guardrail transition and full-scale vehicle crash tested. The W-beam to thrie beam transition element was constructed adjacent to an approved approach guardrail transition which was attached to Missouri's thrie beam and channel bridge railing. Two full-scale vehicle crash tests were performed according to the TL-3 safety performance criteria presented in NCHRP Report No. 350. A summary of the safety performance evaluation for both tests is provided in Table 3. The first crash test, test no. MWT-1, was performed with a small car impacting the transition element and was determined to be acceptable according to the safety performance criteria presented in NCHRP Report No. 350. Following the successful crash test with the small car, the system was repaired and made ready for the final crash test.

A second test, test no. MWT-2, was performed on the W-beam to thrie beam transition element with a ¾-ton pickup truck. During vehicle redirection, the pickup truck rolled onto its side, and the test was determined to be unacceptable according to the safety performance criteria presented in NCHRP Report No. 350. Following an analysis and review of the pickup truck test results, two conditions were observed that were believed to contribute to the poor impact performance. First, considerable torsional collapse was found to occur to post nos. 6 through 8 which were the W152x13.4 steel posts supporting the W-beam to thrie beam transition element. This torsional collapse resulted in reduced lateral support for the guardrail as well as increased penetration into the barrier system. Second, significant vehicle pocketing occurred due to the increased penetration as well as the rapid change in barrier stiffness, resulting in the vehicle climbing the rail and rolling onto its side.

In recent years, the general design methodology of approach guardrail transitions has changed in order to meet the NCHRP Report No. 350 impact safety standards. This change in methodology, based on several crash test programs, has resulted in approach guardrail transitions having increased lateral stiffness. As a result, it may be necessary to provide a more gradual change in stiffness between the W-beam to thrie beam transition element and the existing thrie beam approach guardrail transitions.

Table 3. Summary of Safety Performance Evaluation Results - W-beam to Thrie Beam Transition Section

Evaluation Factors	Evaluation Criteria	Test MWT-1	Test MWT-2
Structural Adequacy	A. Test article should contain and redirect the vehicle; the vehicle should not penetrate, underide, or override the installation although controlled lateral deflection of the test article is acceptable.	S	U
Occupant Risk	D. Detached elements, fragments or other debris from the test article should not penetrate or show potential for penetrating the occupant compartment, or present an undue hazard to other traffic, pedestrians, or personnel in a work zone. Deformations of, or intrusions into, the occupant compartment that could cause serious injuries should not be permitted.	S	S
	F. The vehicle should remain upright during and after collision although moderate roll, pitching and yawing are acceptable.	S	U
	H. Longitudinal and lateral occupant impact velocities should fall below the preferred value of 9 m/s, or at least below the maximum allowable value of 12 m/s.	S	S ¹
	I. Longitudinal and lateral occupant ridedown accelerations should fall below the preferred value of 15 g's, or at least below the maximum allowable value of 20 g's.	S	S ¹
Vehicle Trajectory	K. After collision it is preferable that the vehicle's trajectory not intrude into adjacent traffic lanes.	M	M
	L. The occupant impact velocity in the longitudinal direction should not exceed 12 m/sec and the occupant ridedown acceleration in the longitudinal direction should not exceed 20 G's.	S ¹	S
	M. The exit angle from the test article preferably should be less than 60 percent of test impact angle, measured at time of vehicle loss of contact with test devise.	S	S

S - Satisfactory
M - Marginal
U - Unsatisfactory

¹ Results of evaluation reported here even though it is not required by NCHRP Report No. 350 (4)

10 RECOMMENDATIONS

The W-beam to thrie beam transition element, as described in this report, was not successfully crash tested according to the criteria found in NCHRP Report No. 350. The results of the second crash test with a pickup truck indicate that this design is not a suitable design for use on Federal-aid highways since the vehicle experienced rollover.

Although the W-beam to thrie beam transition element did not perform in an acceptable manner, there still exists the potential for the transition element to meet the TL-3 safety standards. It is likely that simple modifications will greatly improve the system's performance. Examples of these design modifications include the following and/or combinations thereof: (1) incorporating a stiffened W-beam guardrail section upstream of the W-beam to thrie beam transition section; (2) increasing the length of thrie beam between the W-beam to thrie beam transition section and the bridge railing; and (3) incorporating a more gradual change in lateral barrier stiffness near the W-beam to thrie beam transition section. However, any design modifications made to the W-beam to thrie beam transition element or the adjacent barrier system can only be verified through the use of full-scale vehicle crash testing.

11 REFERENCES

1. Bryden, J.E. and Phillips, R.G., *Performance of a Thrie-Beam Steel-Post Bridge-Rail System*, Report No. FHWA/NY/RR-85/118, Submitted to the Office of Research, Development, and Technology, Federal Highway Administration, Performed by New York State Department of Transportation, February 1985.
2. Bryden, J.E. and Phillips, R.G., *Performance of a Thrie-Beam Steel-Post Bridge-Rail System*, Transportation Research Record No. 1024, Transportation Research Board, Washington, D.C., 1985.
3. Michie, J.D., *Recommended Procedures for the Safety Performance Evaluation of Highway Appurtenances*, National Cooperative Highway Research Program (NCHRP) Report No. 230, Transportation Research Board, Washington, D.C., March 1981.
4. Ross, H.E., Sicking, D.L., Zimmer, R.A. and Michie, J.D., *Recommended Procedures for the Safety Performance Evaluation of Highway Features*, National Cooperative Research Program (NCHRP) Report No. 350, Transportation Research Board, Washington, D.C., 1993.
5. *Standard Specifications for Transportation Materials and Methods of Sampling and Testing*, Seventeenth Edition, Part I Specifications, American Association of State Highway and Transportation Officials (AASHTO), Washington, D.C., 1995.
6. Polivka, K.A., Faller, R.K., Reid, J.D., Sicking, D.L., Rohde, J.R., Keller, E.A., and Holloway, J.C., *Development of an Approach Guardrail Transition Attached to a Thrie Beam and Channel Bridge Railing*, Draft Report to the Midwest States Regional Pooled Fund Program, Project SPR-3(017), Transportation Report No. TRP-03-91-99, Midwest Roadside Safety Facility, University of Nebraska-Lincoln, October 14, 1999.
7. *Memorandum on Crash Testing of Bridge Railings*, May 30, 1997, File Designation HNG-14, Federal Highway Administration (FHWA), Washington, D.C., 1997.
8. Hinch, J., Yang, T-L, and Owings, R., *Guidance Systems for Vehicle Testing*, ENSCO, Inc., Springfield, VA 1986.
9. Center of Gravity Test Code - SAE J874 March 1981, SAE Handbook Vol. 4, Society of Automotive Engineers, Inc., Warrendale, Pennsylvania, 1986.
10. Powell, G.H., *BARRIER VII: A Computer Program For Evaluation of Automobile Barrier Systems*, Prepared for: Federal Highway Administration, Report No. FHWA RD-73-51, April 1973.

11. *Vehicle Damage Scale for Traffic Investigators*, Second Edition, Technical Bulletin No. 1, Traffic Accident Data (TAD) Project, National Safety Council, Chicago, Illinois, 1971.
12. *Collision Deformation Classification - Recommended Practice J224 March 1980*, Handbook Volume 4, Society of Automotive Engineers (SAE), Warrendale, Pennsylvania, 1985.

12 APPENDICES

APPENDIX A

Typical BARRIER VII Input File

Note that the example BARRIER VII input data file included in Appendix A corresponds with the critical impact point for tests MWT-1 and MWT-2.

CIP Determination for W-Beam, Thrie-Beam Transition

90	7	4	1	114	26	4	0			
0.0001	0.0001			0.090		500		1.0		1
10	10	10	10	10	0	0				
1	0.0		0.0							
2	0.0		0.0							
3	9.375		0.0							
10	75.		0.0							
34	375.		0.0							
58	600.		0.0							
90	900.0		0.0							
3	10	6	1							
10	34	23	1							
34	58	23	1							
58	90	31	1							
1	50	0.30								
75	74	73	72	71	70	69	68	67	66	
65	64	63	62	61	60	59	58	57	56	
55	54	53	52	51	50	49	48	47	46	
45	44	43	42	41	40	39	38	37	36	
35	34	33	32	31	30	29	28	27	26	
100	12									
1	2.33	1.99		9.375		30000.	6.77	99.5	68.5	0.05
2	2.33	1.99		12.5		30000.	6.77	99.5	68.5	0.05
3	2.3905	2.0600		9.375		30000.0	7.166	103.00	76.07	0.05
4	2.5716	2.2001		9.375		30000.0	7.657	110.00	81.12	0.05
5	2.7526	2.3402		9.375		30000.0	8.148	117.0	86.17	0.05
6	2.9337	2.4803		9.375		30000.0	8.639	124.0	91.21	0.05
7	3.1148	2.6204		9.375		30000.0	9.130	131.0	96.26	0.05
8	3.2958	2.7605		9.375		30000.0	9.621	138.0	101.31	0.05
9	3.4768	2.9006		9.375		30000.0	10.112	145.00	106.35	0.05
10	3.6580	3.0407		9.375		30000.0	10.603	152.0	108.88	0.05
11	7.52	6.20		9.375		30000.0	21.62	310.0	219.0	0.05
12	29.6	3.89		9.375		30000.0	13.25	5.0	436.54	0.05
200	1									
1	0.334	59.0		30000.		0.90	50.0	0.05		
300	8									
1	21.65	3.		3.56		4.55	51.	10000.	10000.	0.05
	BCT End Post									
10000.	10000.	10000.	10000.							
2	21.65	0.		5.0		3.75	51.	10000.	10000.	0.05
	BCT Second Post									
11.0	14.7	10000.		10000.						
3	21.65	0.0		4.00		4.00	54.0	92.88	270.62	0.05
	W6x9 by 6' Long									
	6.0	15.0		16.0		16.0				
4	21.65	0.0		4.00		4.00	58.5	92.88	270.62	0.10
	W6x9 by 6.5' Long									
	6.0	15.0		16.0		16.0				
5	21.65	0.0		8.0		8.0	105.0	256.5	539.52	0.05
	W6x15 by 7' Long									
	15.0	30.0		16.0		16.0				
6	21.65	26.00		8.0		8.0	105.0	256.5	539.52	0.05
	W6x15 by 7' Long with channel at 26 in.									
	15.0	30.0		16.0		16.0				
7	21.65	33.00		8.0		8.0	105.0	256.5	539.52	0.05
	W6x15 by 7' Long with channel at 33 in.									
	15.0	30.0		16.0		16.0				

	8	21.65	33.00	1000.0	1000.0	250.0	10000.0	10000.0	0.05
		Strong Post Anchor with channel at 33 in.							
		200.0	200.0	2.0	2.0				
400	1								
	1	50.	2.0	3.0	6.6	100.	0.10	5.0	
	1	1	3	2	101	0.	0.	0.	
	2	3	4	6	1	101	0.	0.	
	7	8	9		1	401			
	8	9	10		1	101			
	9	10	11	32	1	102	0.	0.	
	33	34	35	56	1	101			
	57	58	59		1	103			
	58	59	60		1	104			
	59	60	61		1	105			
	60	61	62		1	106			
	61	62	63		1	107			
	62	63	64		1	108			
	63	64	65		1	109			
	64	65	66		1	110			
	65	66	67	88	1	111			
	89	82	83	96	1	112			
	97	2	8		6	201	0.	0.	
	98	1	2			301	0.	0.	0.
	99	10				302			
	100	16	103		6	303			
	104	42	106		8	303			
	107	62	108		4	304			
	109	70	111		4	305			
	112	82				306			
	113	86				307			
	114	90				308			
1965.		17000.		13	1	4	0	3	
	1	0.025	0.150	4.5		10.			
	1	35.0	24.		1	1.0	0	0	0
	2	35.0	-24.		1	1.0	0	0	0
	3	-83.	30.		1	40.	1	0	0
	4	-40.	30.		1	40.	1	0	0
	5	0.0	30.		1	20.	1	0	0
	6	20.0	30.		1	20.	1	0	0
	7	40.	30.		1	20.	1	0	0
	8	61.	30.		1	20.	1	0	0
	9	61.	15.		1	15.	1	0	0
	10	61.	0.0		1	15.	1	0	0
	11	61.	-15.		1	15.	1	0	0
	12	61.	-30.		1	20.	1	0	0
	13	-83.	-30.		1	20.	0	0	0
	1	35.	24.	0.		400.			
	2	35.	-24.	0.		400.			
	3	-52.	24.	0.		300.			
	4	-52.	-24.	0.		300.			
	1	0.0	0.0						
	2	61.	30.						
	3	35.	24.						
	8	570.	0.0	20.0		62.14	0.0	0.0	0.0

CIP Determination for W-Beam, Thrie-Beam Transition - 2000P Vehicle

90	7	4	1	114	26	4	0			
0.0001	0.0001		0.175		500		1.0		1	
10	10	10	10	0	0					
1	0.0		0.0							
2	0.0		0.0							
3	9.375		0.0							
10	75.		0.0							
34	375.		0.0							
58	600.		0.0							
90	900.0		0.0							
3	10	6	1							
10	34	23	1							
34	58	23	1							
58	90	31	1							
1	50	0.30								
75	74	73	72	71	70	69	68	67	66	
65	64	63	62	61	60	59	58	57	56	
55	54	53	52	51	50	49	48	47	46	
45	44	43	42	41	40	39	38	37	36	
35	34	33	32	31	30	29	28	27	26	
100	12									
1	2.33	1.99	9.375	30000.	6.77	99.5	68.5	0.05		
2	2.33	1.99	12.5	30000.	6.77	99.5	68.5	0.05		
3	2.3905	2.0600	9.375	30000.0	7.166	103.00	76.07	0.05		
4	2.5716	2.2001	9.375	30000.0	7.657	110.00	81.12	0.05		
5	2.7526	2.3402	9.375	30000.0	8.148	117.0	86.17	0.05		
6	2.9337	2.4803	9.375	30000.0	8.639	124.0	91.21	0.05		
7	3.1148	2.6204	9.375	30000.0	9.130	131.0	96.26	0.05		
8	3.2958	2.7605	9.375	30000.0	9.621	138.0	101.31	0.05		
9	3.4768	2.9006	9.375	30000.0	10.112	145.00	106.35	0.05		
10	3.6580	3.0407	9.375	30000.0	10.603	152.0	108.88	0.05		
11	7.52	6.20	9.375	30000.0	21.62	310.0	219.0	0.05		
12	29.6	3.89	9.375	30000.0	13.25	5.0	436.54	0.05		
200	1									
1	0.334	59.0	30000.	0.90	50.0	0.05				
300	8									
1	21.65	3.	3.56	4.55	51.	10000.	10000.	0.05		
	BCT End Post									
10000.	10000.	10000.	10000.							
2	21.65	0.	5.0	3.75	51.	10000.	10000.	0.05		
	BCT Second Post									
11.0	14.7	10000.	10000.							
3	21.65	0.0	4.00	4.00	54.0	92.88	270.62	0.05		
	W6x9 by 6' Long									
	6.0	15.0	16.0	16.0						
4	21.65	0.0	4.00	4.00	58.5	92.88	270.62	0.10		
	W6x9 by 6.5' Long									
	6.0	15.0	16.0	16.0						
5	21.65	0.0	8.0	8.0	105.0	256.5	539.52	0.05		
	W6x15 by 7' Long									
	15.0	30.0	16.0	16.0						
6	21.65	26.00	8.0	8.0	105.0	256.5	539.52	0.05		
	W6x15 by 7' Long with channel at 26 in.									
	15.0	30.0	16.0	16.0						
7	21.65	33.00	8.0	8.0	105.0	256.5	539.52	0.05		
	W6x15 by 7' Long with channel at 33 in.									
	15.0	30.0	16.0	16.0						

8	21.65	33.00	1000.0	1000.0	250.0	10000.0	10000.0	0.05
Strong Post Anchor with channel at 33 in.								
200.0	200.0	2.0	2.0	2.0				
400	1							
1	50.	2.0	3.0	6.6	100.	0.10	5.0	
1	1	3	2	101	0.	0.	0.	
2	3	4	6	1	101	0.	0.	
7	8	9	1	401				
8	9	10	1	101				
9	10	11	32	1	102	0.	0.	0.
33	34	35	56	1	101			
57	58	59	1	103				
58	59	60	1	104				
59	60	61	1	105				
60	61	62	1	106				
61	62	63	1	107				
62	63	64	1	108				
63	64	65	1	109				
64	65	66	1	110				
65	66	67	88	1	111			
89	82	83	96	1	112			
97	2	8	6	201	0.	0.		
98	1	2		301	0.	0.	0.	0.
99	10			302				
100	16	103	6	303				
104	42	106	8	303				
107	62	108	4	304				
109	70	111	4	305				
112	82			306				
113	86			307				
114	90			308				
4400.0	40000.0	20	6	4	0	3		
1	0.055	0.12		6.00		17.0		
2	0.057	0.15		7.00		18.0		
3	0.062	0.18		10.00		12.0		
4	0.110	0.35		12.00		6.0		
5	0.35	0.45		6.00		5.0		
6	1.45	1.50		15.00		1.0		
1	100.75	15.875	1	12.0	1	0	0	0
2	100.75	27.875	1	12.0	1	0	0	0
3	100.75	39.875	2	12.0	1	0	0	0
4	88.75	39.875	2	12.0	1	0	0	0
5	76.75	39.875	2	12.0	1	0	0	0
6	64.75	39.875	2	12.0	1	0	0	0
7	52.75	39.875	2	12.0	1	0	0	0
8	40.75	39.875	2	12.0	1	0	0	0
9	28.75	39.875	2	12.0	1	0	0	0
10	16.75	39.875	2	12.0	1	0	0	0
11	-13.25	39.875	3	12.0	1	0	0	0
12	-33.25	39.875	3	12.0	1	0	0	0
13	-53.25	39.875	3	12.0	1	0	0	0
14	-73.25	39.875	3	12.0	1	0	0	0
15	-93.25	39.875	3	12.0	1	0	0	0
16	-113.25	39.875	4	12.0	1	0	0	0
17	-113.25	-39.875	4	12.0	0	0	0	0
18	100.75	-39.875	1	12.0	0	0	0	0
19	69.25	37.75	5	1.0	0	0	0	0
20	-62.75	37.75	6	1.0	0	0	0	0

1	69.25	32.75	0.0	608.			
2	69.25	-32.75	0.0	608.			
3	-62.75	32.75	0.0	492.			
4	-62.75	-32.75	0.0	492.			
1	0.0	0.0					
2	100.75	39.875					
3	69.25	32.75					
3	488.00	0.0	25.0	62.14	0.0	0.0	1.0

APPENDIX B

Accelerometer Data Analysis, Test MWT-1

Figure B-1. Graph of Longitudinal Deceleration, Test MWT-1

Figure B-2. Graph of Longitudinal Occupant Impact Velocity, Test MWT-1

Figure B-3. Graph of Longitudinal Occupant Displacement, Test MWT-1

Figure B-4. Graph of Lateral Deceleration, Test MWT-1

Figure B-5. Graph of Lateral Occupant Impact Velocity, Test MWT-1

Figure B-6. Graph of Lateral Occupant Displacement, Test MWT-1

W17: Longitudinal Deceleration - 10-Msec Avg. - Filtered Data - Test MWT-1 (EDR-4)

96

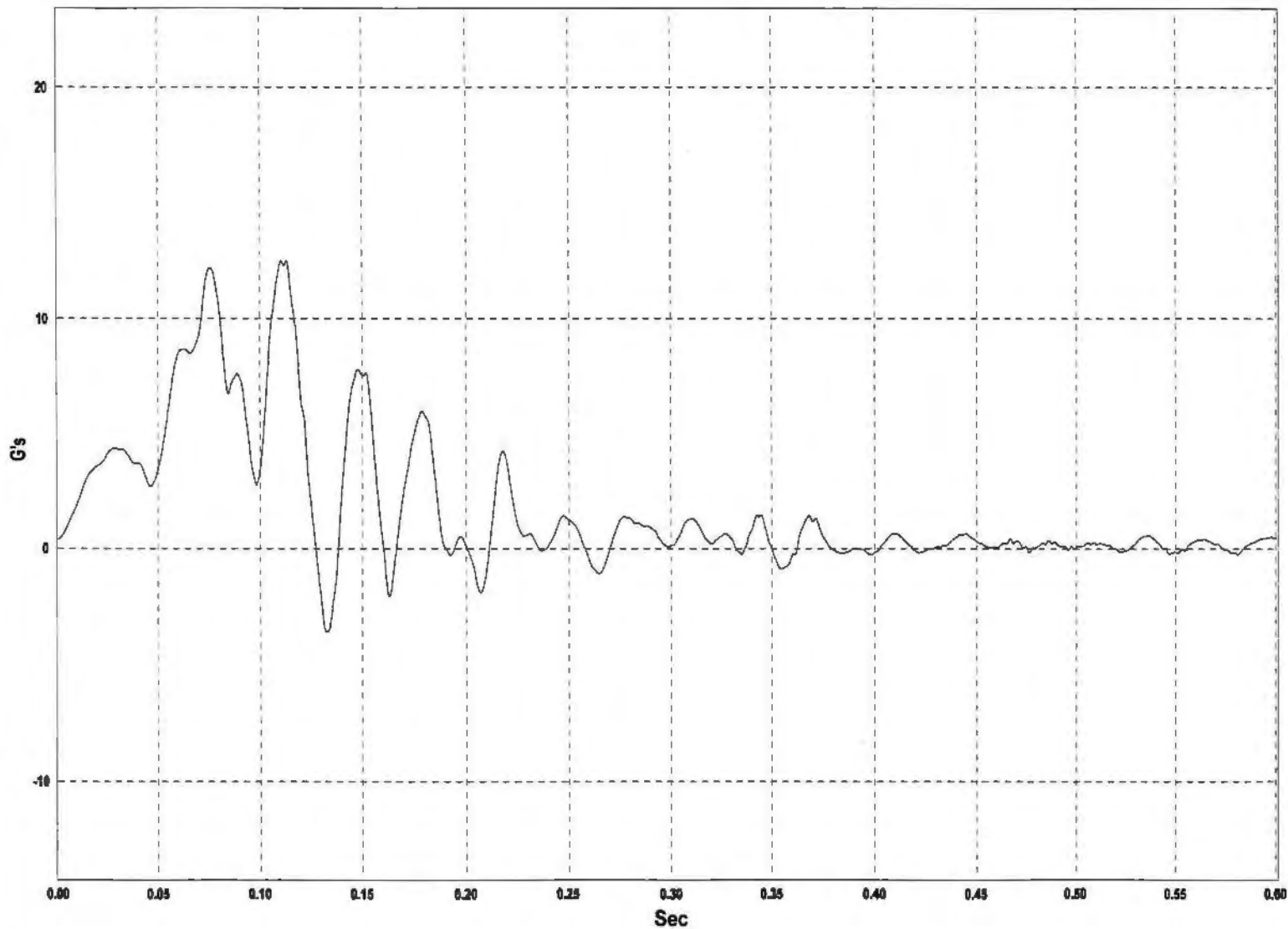


Figure B-1. Graph of Longitudinal Deceleration, Test MWT-1

W8: Longitudinal Occupant Impact Velocity - Filtered Data - Test MWT-1 (EDR-4)

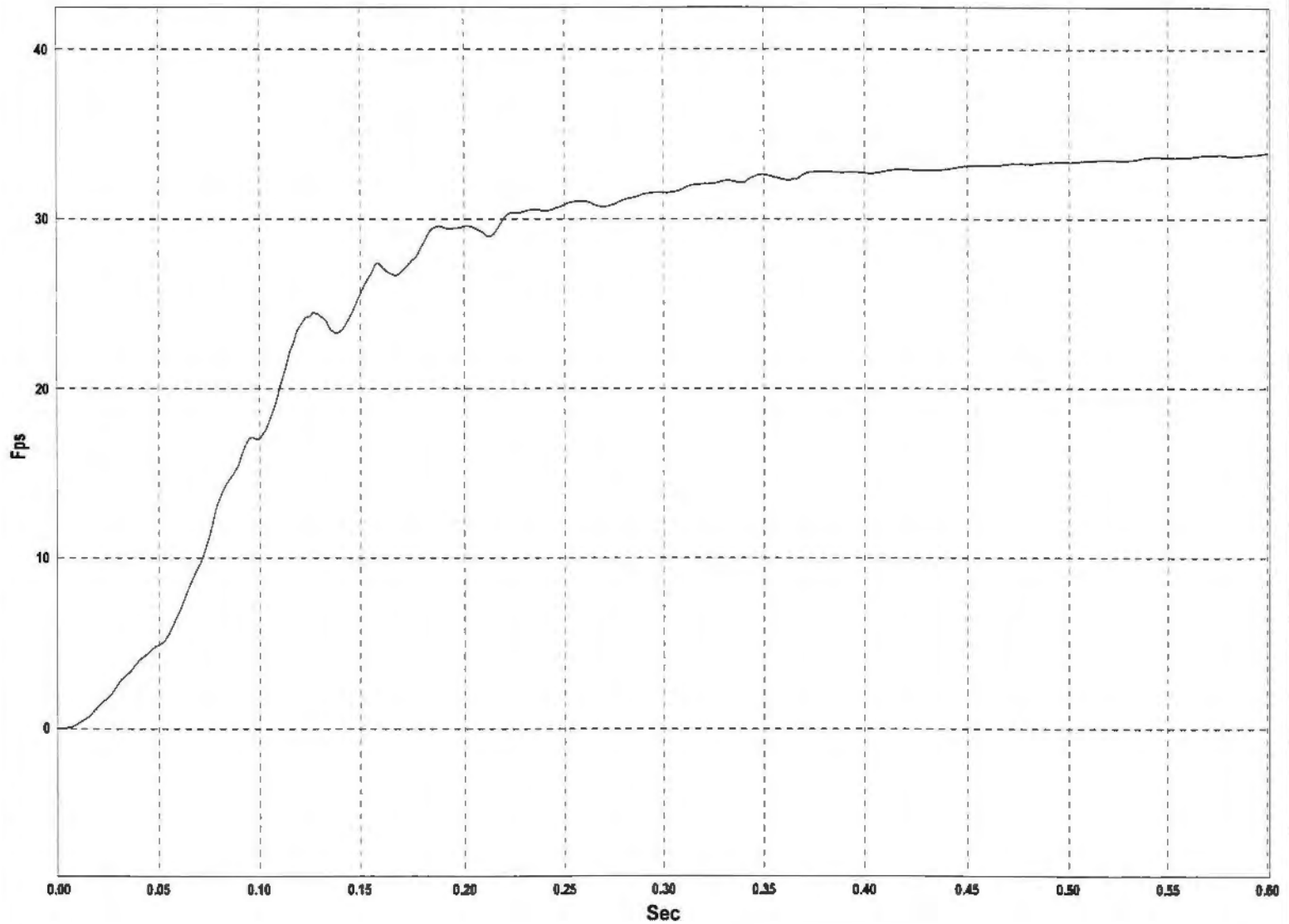


Figure B-2. Graph of Longitudinal Occupant Impact Velocity, Test MWT-1

W9: Longitudinal Occupant Displacement - Filtered Data - Test MWT-1 (EDR-4)

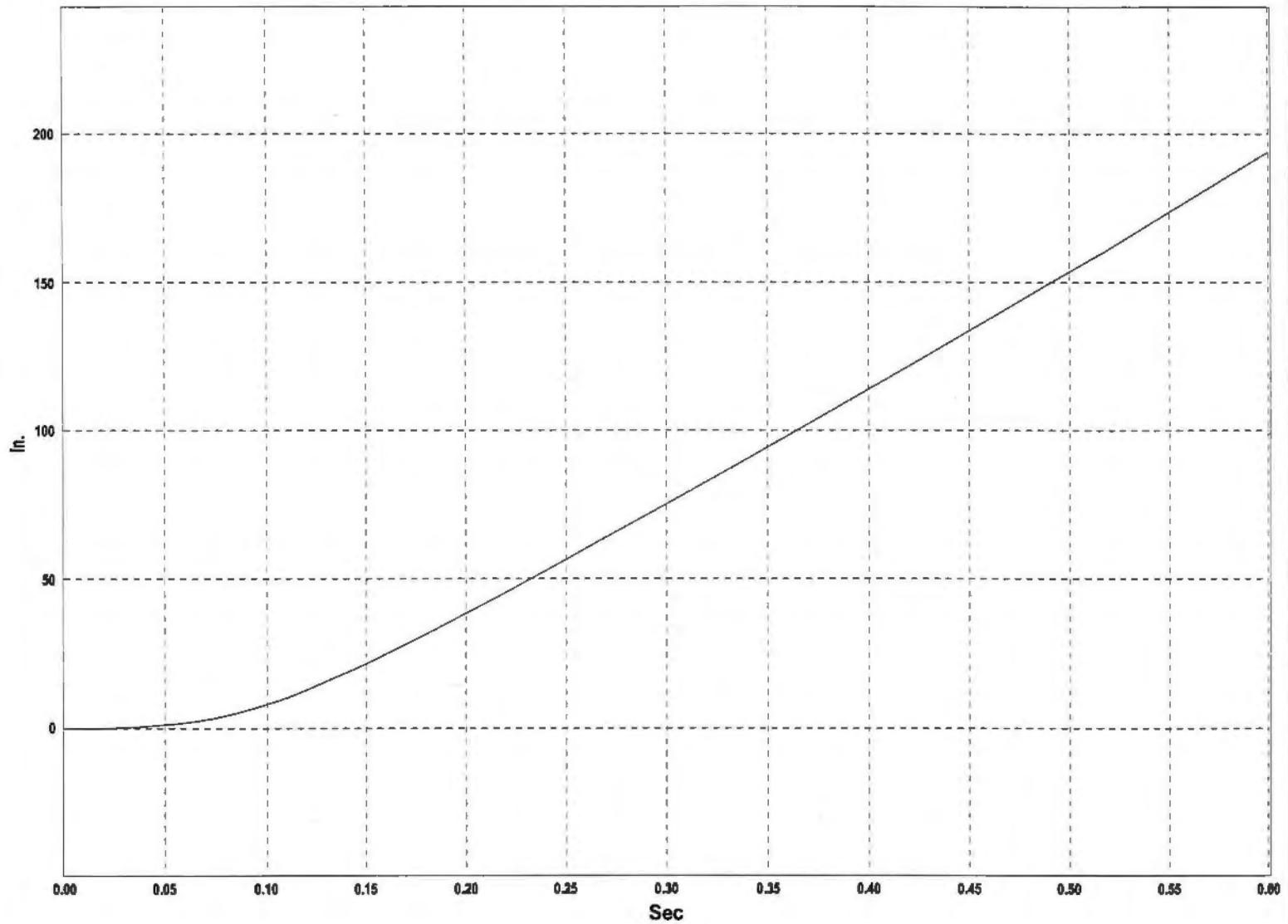
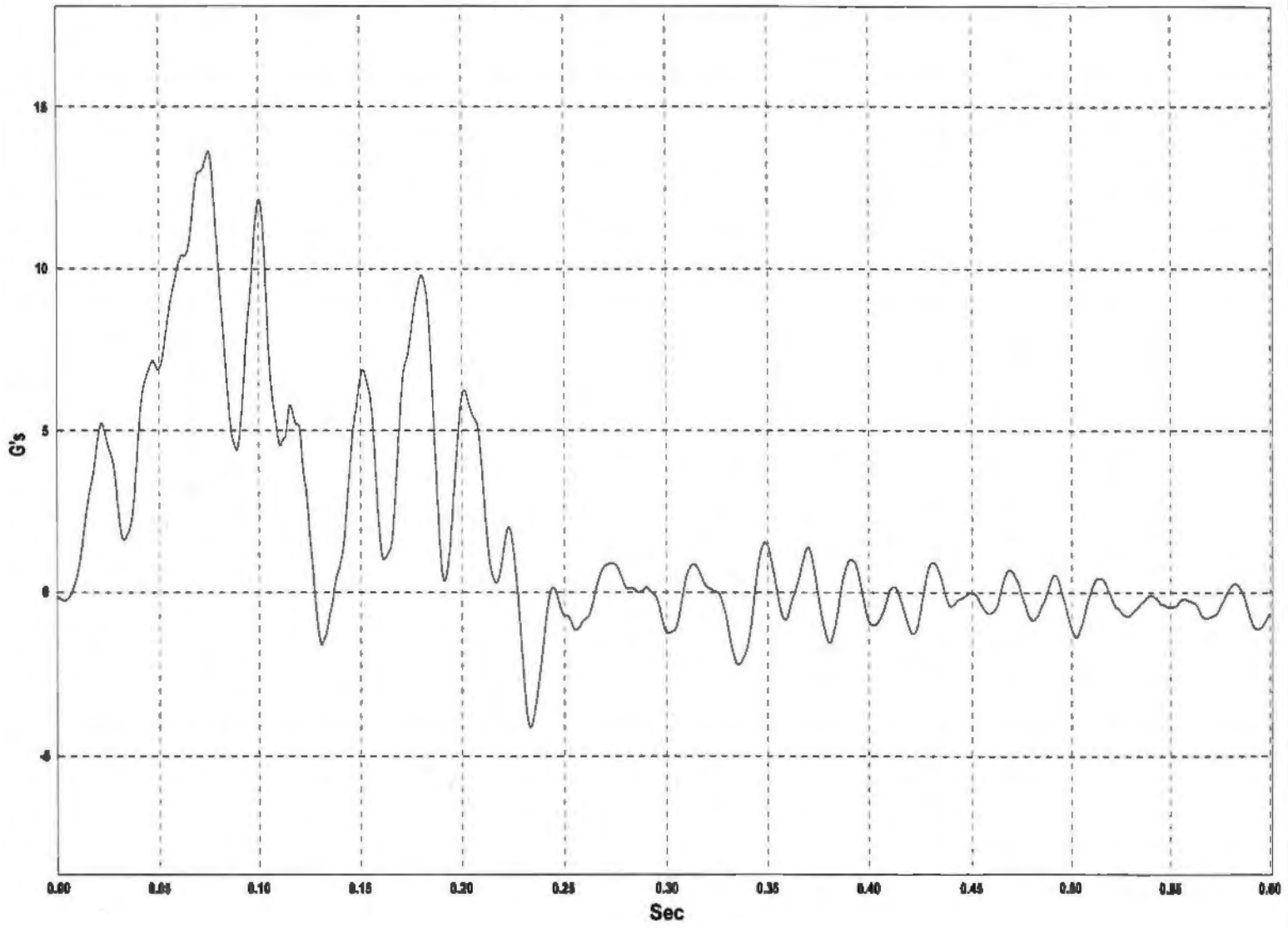


Figure B-3. Graph of Longitudinal Occupant Displacement, Test MWT-1

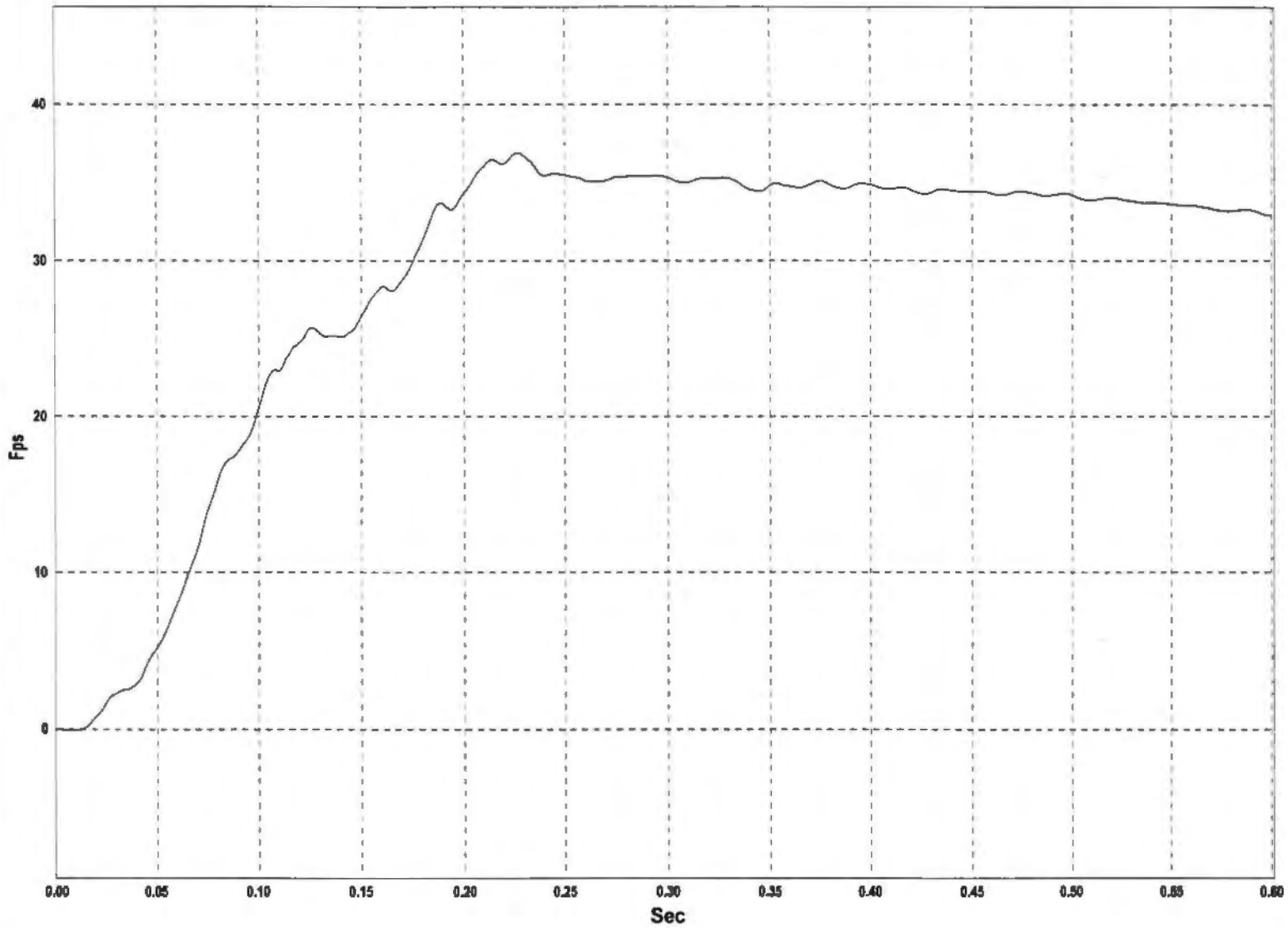
W12: Lateral Deceleration - 10-Msec Avg. - Filtered Data - Test MWT-1 (EDR-4)



86

Figure B-4. Graph of Lateral Deceleration, Test MWT-1

W8: Lateral Occupant Impact Velocity - Filtered Data - Test MWT-1 (EDR-4)



66

Figure B-5. Graph of Lateral Occupant Impact Velocity, Test MWT-1

W9: Lateral Occupant Displacement - Filtered Data - Test MWT-1 (EDR-4)

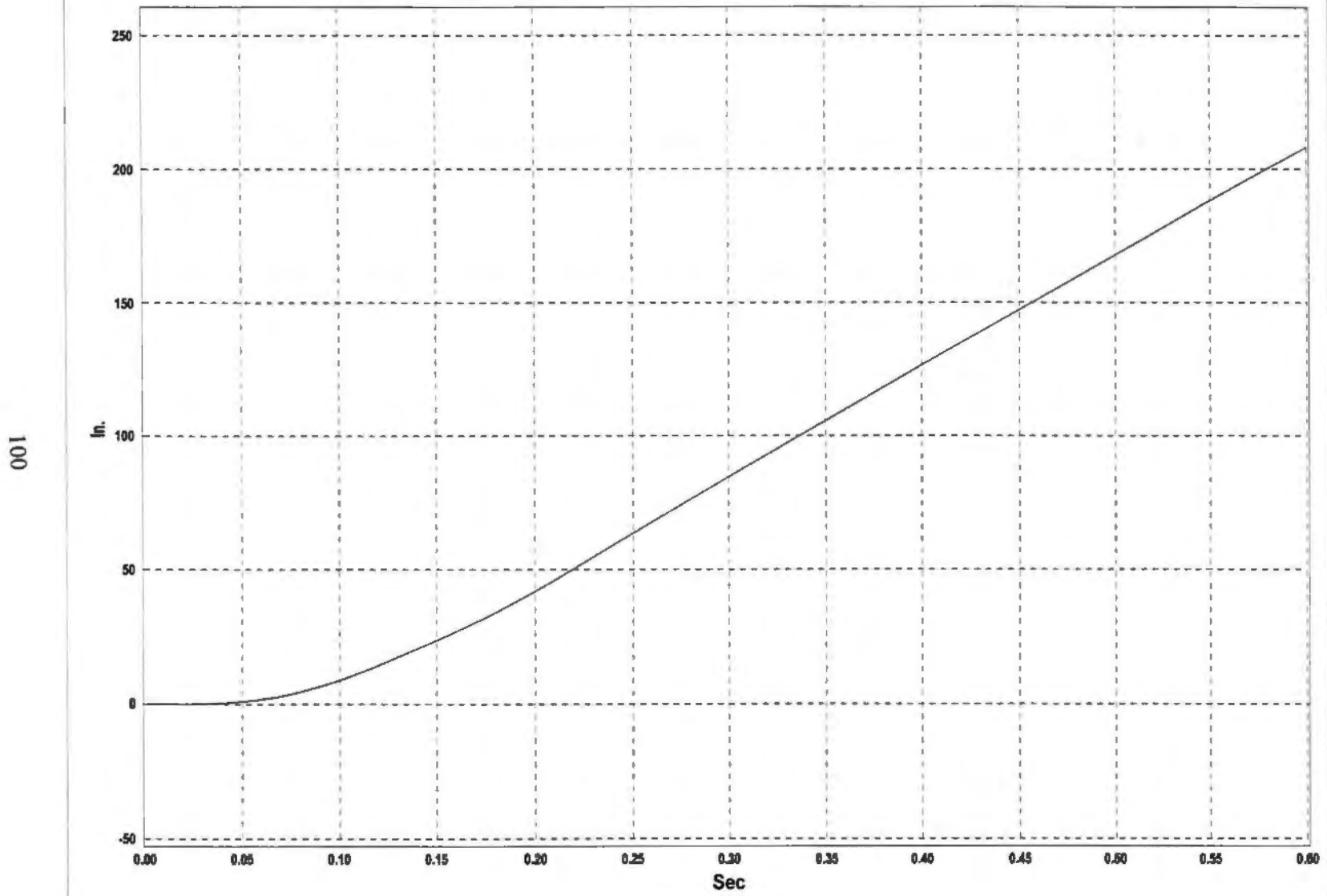


Figure B-6. Graph of Lateral Occupant Displacement, Test MWT-1

APPENDIX C

Rate Transducer Data Analysis, Test MWT-1

Figure C-1. Graph of Roll, Pitch, and Yaw Angular Displacements, Test MWT-1

W19: TEST MWT-1 UNCOUPLED ANGULAR DISPLACEMENTS

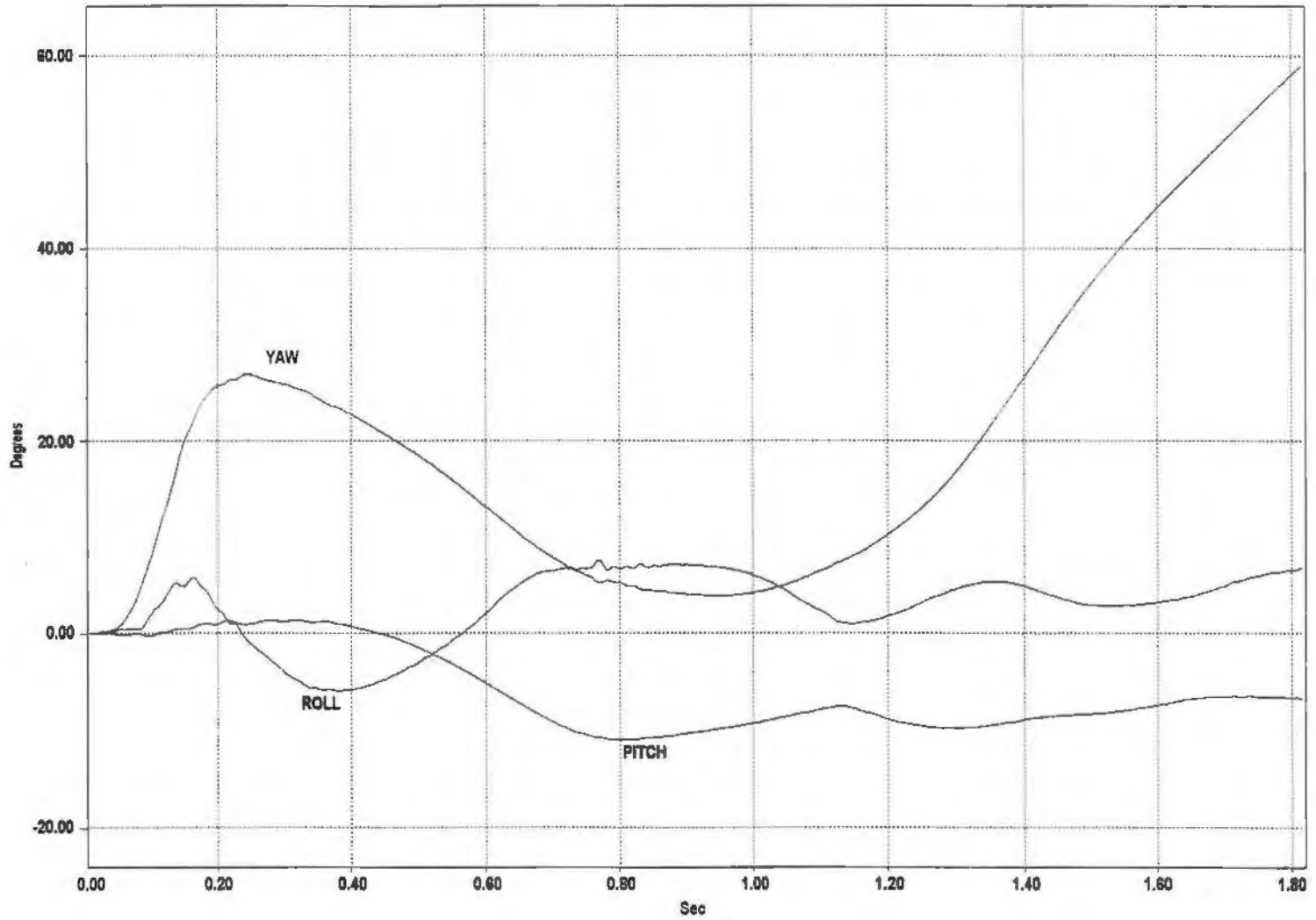


Figure C-1. Graph of Roll, Pitch, and Yaw Angular Displacements, Test MWT-1

APPENDIX D

Accelerometer Data Analysis, Test MWT-2

Figure D-1. Graph of Longitudinal Decelerations, Test MWT-2

Figure D-2. Graph of Longitudinal Occupant Impact Velocity, Test MWT-2

Figure D-3. Graph of Longitudinal Occupant Displacement, Test MWT-2

Figure D-4. Graph of Lateral Deceleration, Test MWT-2

Figure D-5. Graph of Lateral Occupant Impact Velocity, Test MWT-2

Figure D-6. Graph of Lateral Occupant Displacement, Test MWT-2

W17: Longitudinal Deceleration - 10-Msec Avg. - Filtered Data - Test MWT-2 (EDR-4)

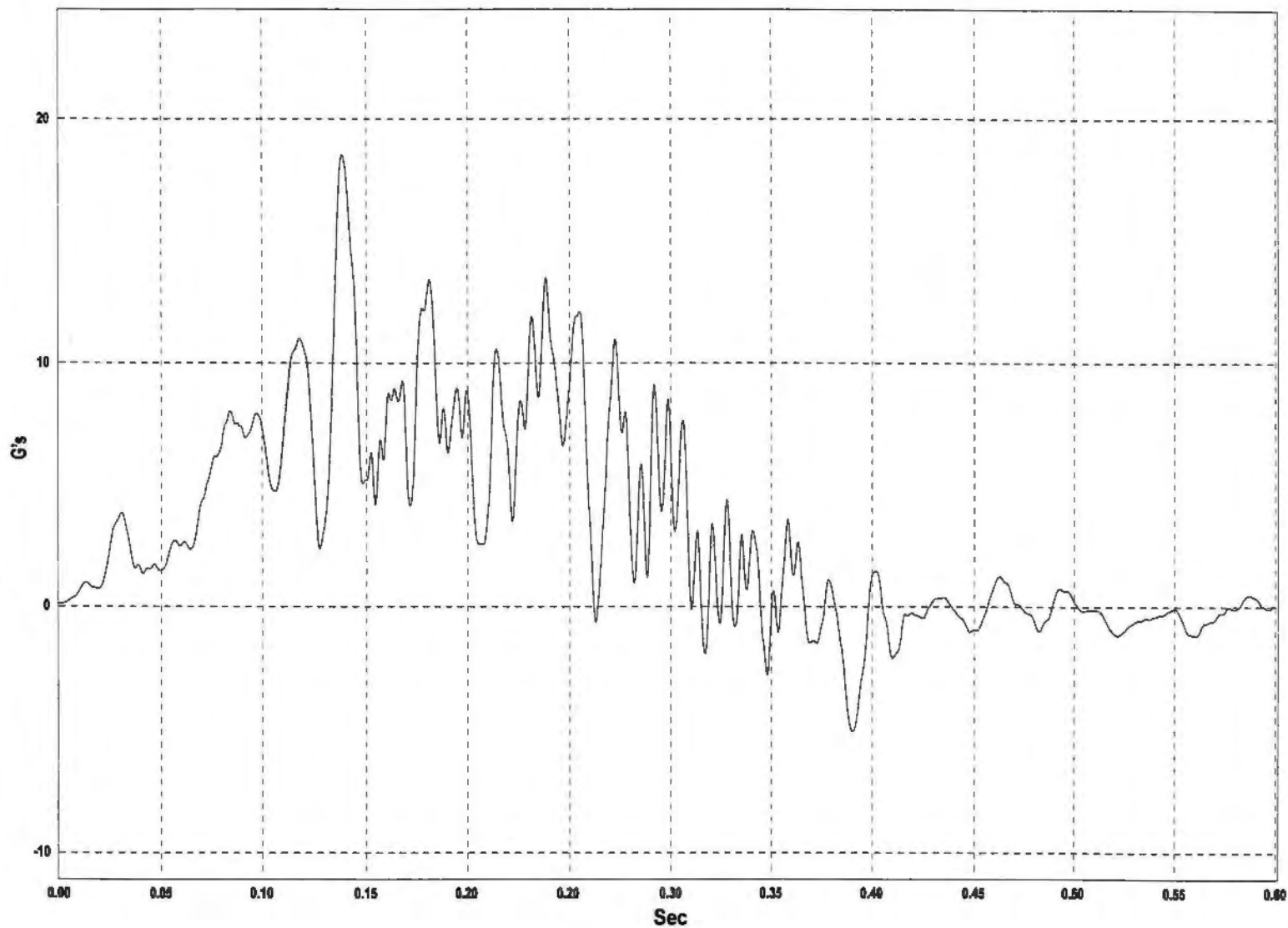
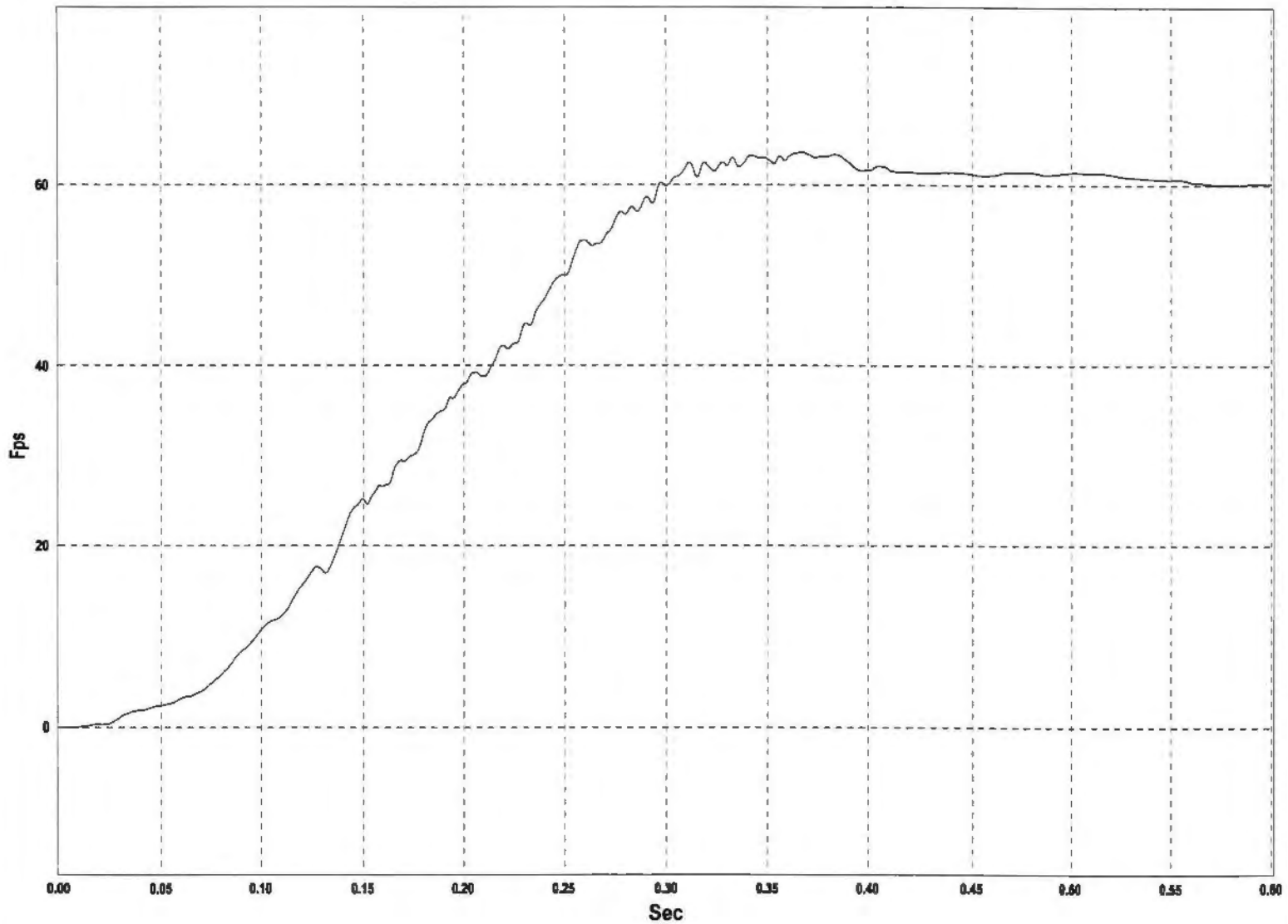


Figure D-1. Graph of Longitudinal Deceleration, Test MWT-2

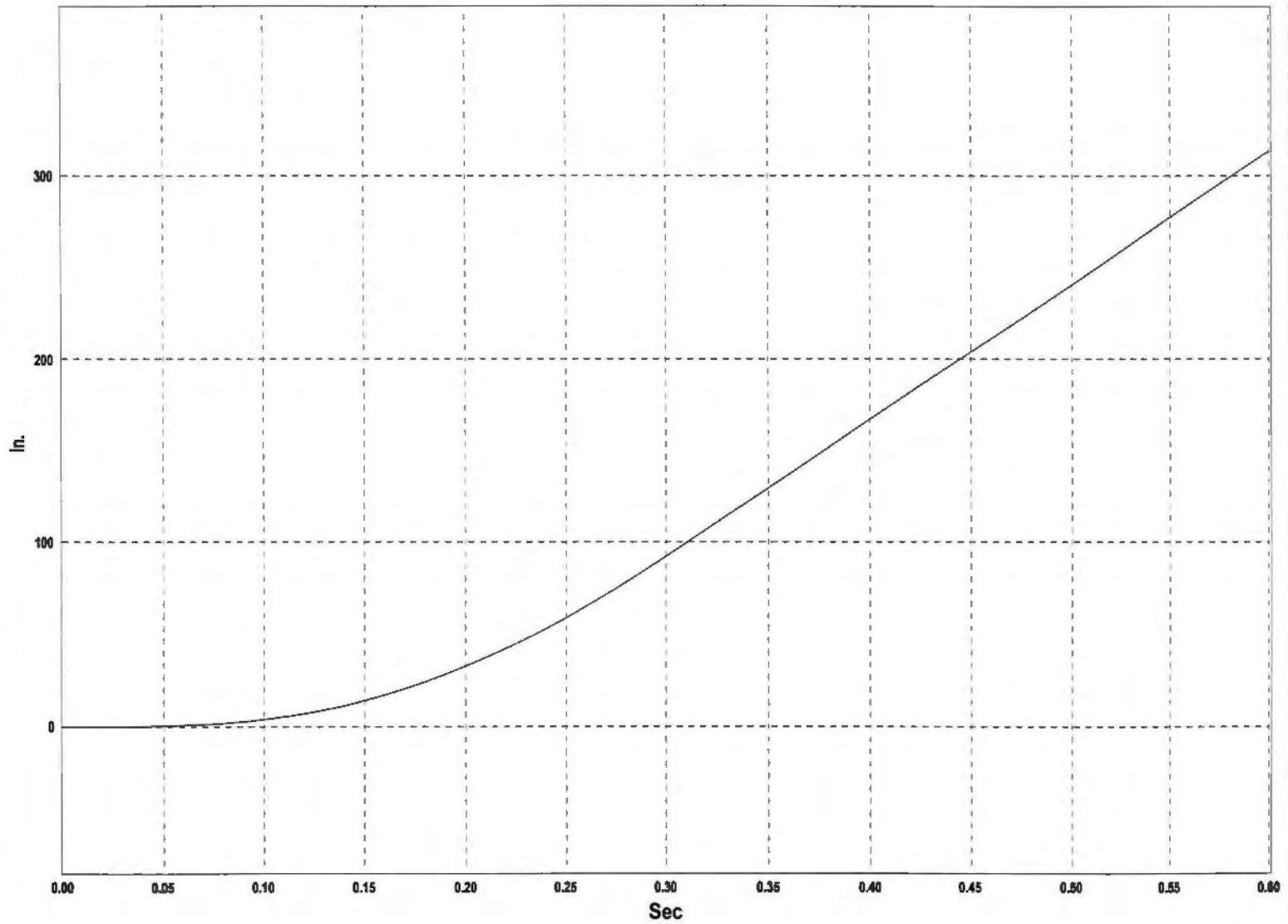
W8: Longitudinal Occupant Impact Velocity - Filtered Data - Test MWT-2 (EDR-4)



105

Figure D-2. Graph of Longitudinal Occupant Impact Velocity, Test MWT-2

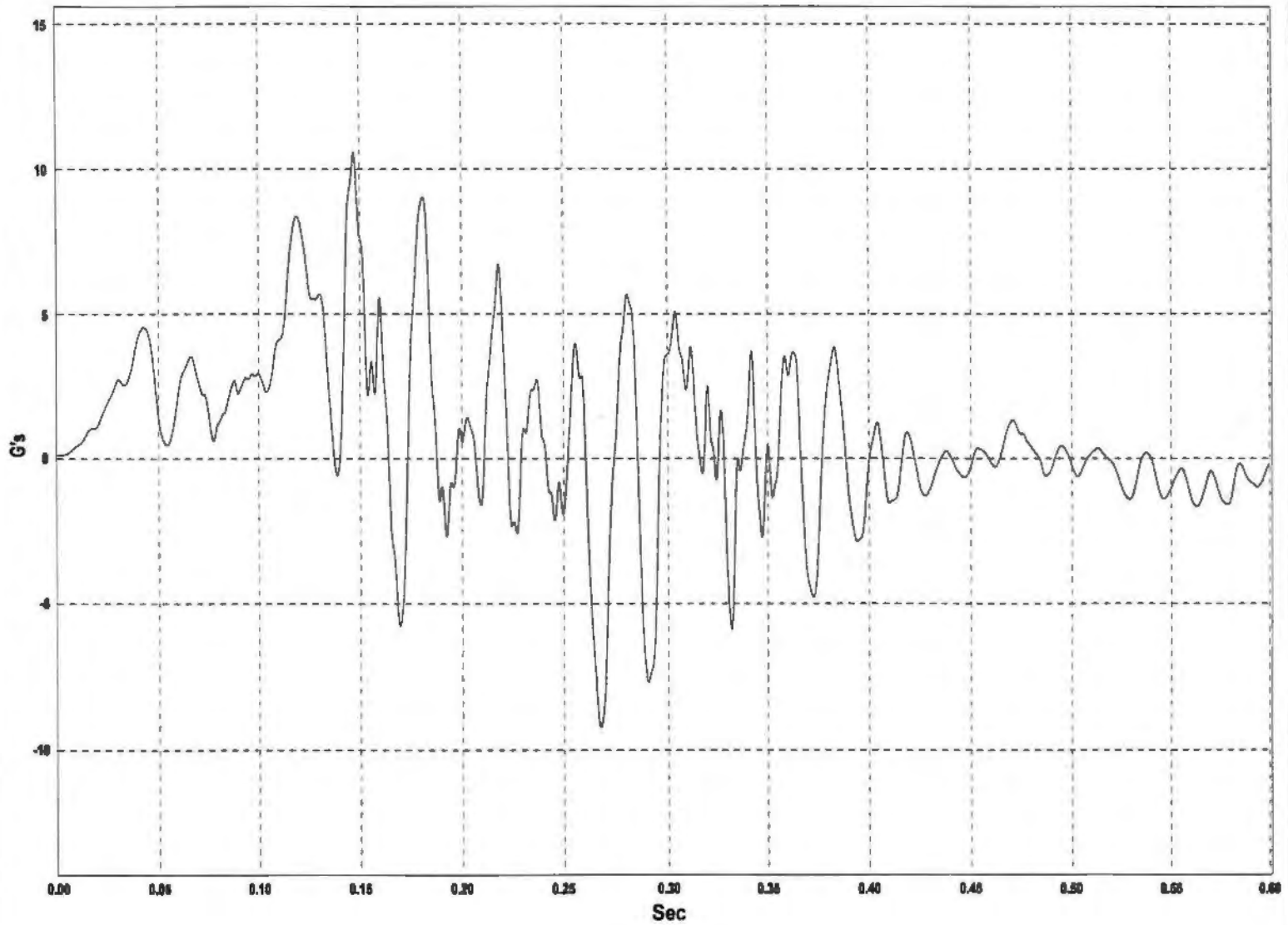
W9: Longitudinal Occupant Displacement - Filtered Data - Test MWT-2 (EDR-4)



106

Figure D-3. Graph of Longitudinal Occupant Displacement, Test MWT-2

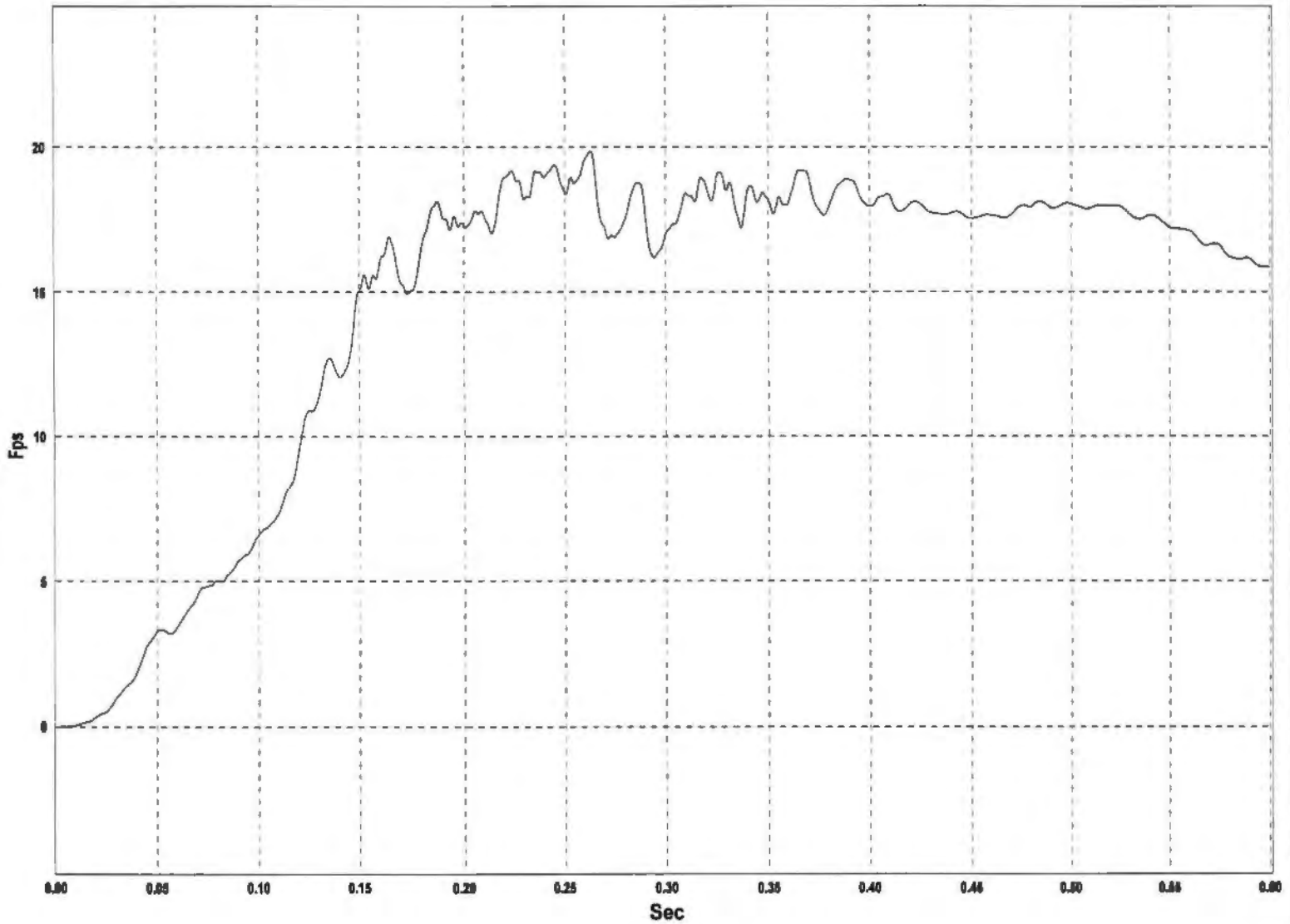
W12: Lateral Deceleration - 10-Msec Avg. - Filtered Data - Test MWT-2 (EDR-4)



107

Figure D-4. Graph of Lateral Deceleration, Test MWT-2

W8: Lateral Occupant Impact Velocity - Filtered Data - Test MWT-2 (EDR-4)



108

Figure D-5. Graph of Lateral Occupant Impact Velocity, Test MWT-2

W9: Lateral Occupant Displacement - Filtered Data - Test MWT-2 (EDR-4)

601

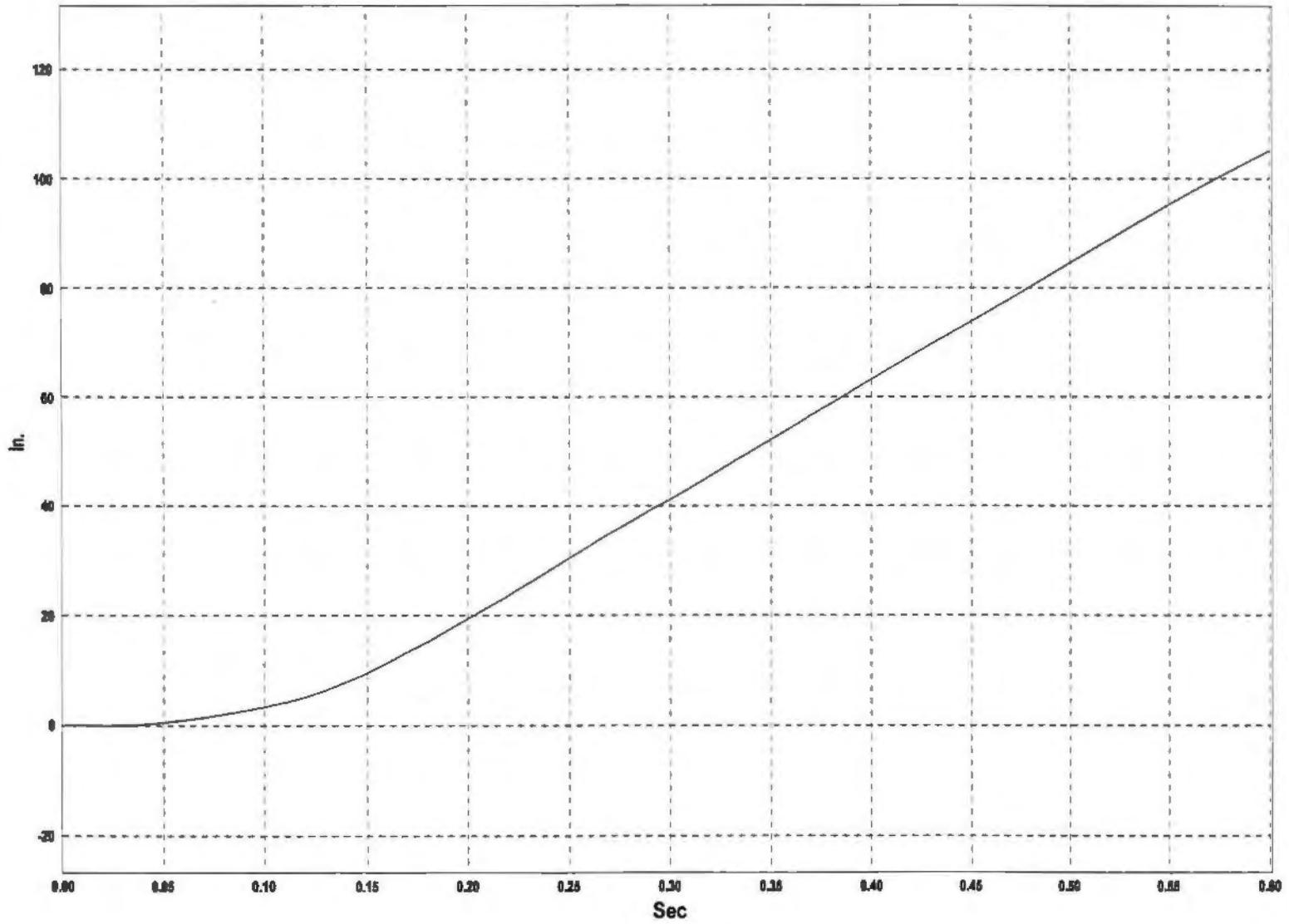


Figure D-6. Graph of Lateral Occupant Displacement, Test MWT-2

APPENDIX E

Rate Transducer Data Analysis, Test MWT-2

Figure E-1. Graph of Roll, Pitch, and Yaw Angular Displacements, Test MWT-2

W19: TEST MWT-2 UNCOUPLED ANGULAR DISPLACEMENTS

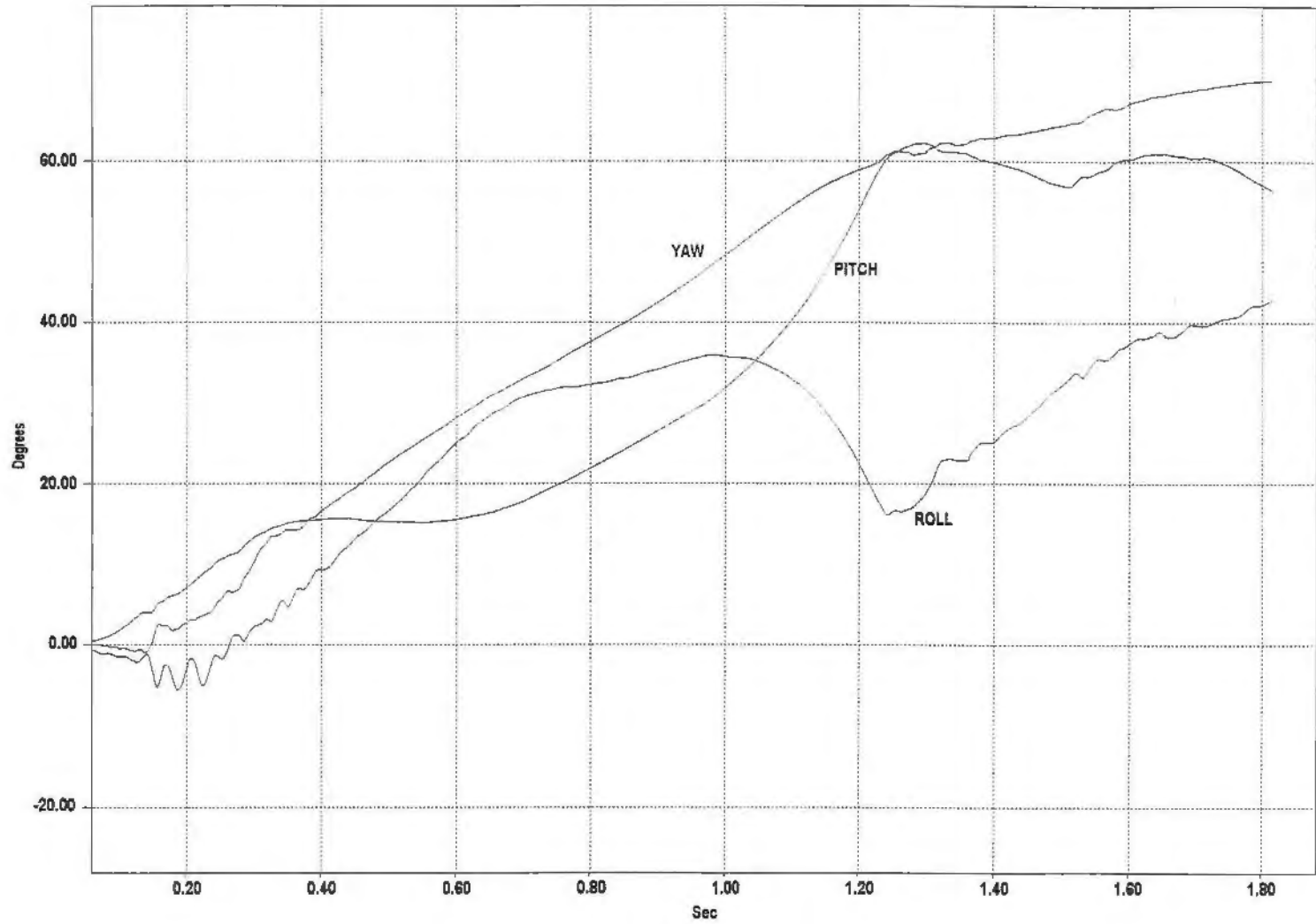


Figure E-1. Graph of Roll, Pitch, and Yaw Angular Displacements, Test MWT-2